
ORIGINAL ARTICLE

Seasonal Count Time Series

Jiajie Kong¹ | Robert Lund²

¹Department of Statistics, University of California, Santa Cruz, Santa Cruz, CA, 95064, United States

²Department of Statistics, University of California, Santa Cruz, Santa Cruz, CA, 95064, United States

Correspondence

Jiajie Kong, Department of Statistics, University of California, Santa Cruz, Santa Cruz, CA, 95064, United States
Email: jkong7@ucsc.edu

Present address

[†]Department of Statistics, University of California, Santa Cruz, Santa Cruz, CA, 95064, United States

Funding information

The authors thank NSF support from Grant DMS 21-13592.

Count time series are widely encountered in practice. As with continuous valued data, many count series have seasonal properties. This paper uses a recent advance in stationary count time series to develop a general seasonal count time series modeling paradigm. The model permits any marginal distribution for the series and the most flexible autocorrelations possible, including those with negative dependence. Likelihood methods of inference can be conducted and covariates can be easily accommodated. The paper first develops the modeling methods, which entail a discrete transformation of a Gaussian process having seasonal dynamics. Properties of this model class are then established and particle filtering likelihood methods of parameter estimation are developed. A simulation study demonstrating the efficacy of the methods is presented and an application to the number of rainy days in successive weeks in Seattle, Washington is given.

KEYWORDS

Copulas, Counts, PARMA Series, Particle Filtering, Periodicity, SARMA Series

1 | INTRODUCTION

Count time series is an active area of current research, with several recent review papers and books appearing on the topic (Fokianos, 2012, Davis et al., 2016, Weiß, 2018, Davis et al., 2021). Gaussian models, which are completely

* Equally contributing authors.

characterized by the series' mean and autocovariance structure, may inadequately describe count series, especially when the counts are small. This paper uses a recent advance in count modeling in Jia et al. (2021) to develop a very general count time series model with seasonal characteristics. Specifically, a transformation technique is used to convert a standardized seasonal correlated Gaussian process into a seasonal count time series. The modeling paradigm allows any marginal count distribution to be produced, has very general correlation structures that can be positive or negative, and can be fitted via likelihood methods. While our most basic setup produces strictly stationary count series (in a periodic sense), nonstationary extensions, particularly those involving covariates, are easily achieved.

With T denoting the known period of the data, our objective is to model a time series $\{X_t\}$ in time t that has a count marginal distribution and periodic properties with known period T . A seasonal notation uses $X_{dT+\nu}$ to denote the series during the ν th season of cycle d . Here, $\nu \in \{1, 2, \dots, T\}$ is the seasonal index and $d \in \{0, 1, 2, n/T - 1\}$. We assume that there are n total observations, taken at the times $1, 2, \dots, n/T$. To avoid trite work with edge effects, we assume that n/T is a whole number.

We seek to construct count series having the cumulative distribution function $F_\nu(x) = P\{X_{dT+\nu} \leq x\}$ for each cycle d — this stipulation imposes a periodic marginal distribution on the series. In fact, our constructed series will be strictly periodically stationary: for each $k \geq 1$ and all times $t_1 < t_2 < \dots < t_k$, the joint distribution of $(X_{t_1}, \dots, X_{t_k})'$ coincides with that of $(X_{t_1+T}, \dots, X_{t_k+T})'$. We use notations such as $\{X_t\}$ and $\{X_{dT+\nu}\}$ interchangeably, the latter being preferred when seasonality is emphasized.

Some previous seasonal count time series models are now reviewed. The most widely used seasonal count time series models to date develop periodic versions of discrete integer-valued autoregressions (PINAR models) — see Monteiro et al. (2010), Santos et al. (2019), and Bentarzi and Aries (2020). For example, a first order PINAR series $\{X_t\}$ obeys the difference equation

$$X_{dT+\nu} = \rho(\nu) \circ X_{dT+\nu-1} + \epsilon_{dT+\nu}.$$

Here, $\rho(\nu) \in [0, 1]$ for each season ν and \circ denotes the classical thinning operator: for an independent and identically distributed (IID) sequence of zero-one Bernoulli trials $\{B_i\}_{i=1}^\infty$ and a count-valued random variable C that is independent of $\{B_i\}_{i=1}^\infty$, $\rho \circ C := \sum_{i=1}^C B_i$. The noises $\{\epsilon_{dT+\nu}\}$ are periodic independent and identically distributed (IID) count-valued random variables having finite second moments.

The PINAR model class has drawbacks. Even in the stationary case, PINAR models cannot produce some marginal distributions. Joe (2016) quantifies the issue in the stationary case, showing that only marginal distributions in the so-called discrete self-decomposable family can be achieved. Another issue is that PINAR models must have non-negative correlations. Negatively correlated count series do arise (Kachour and Yao, 2009, Livsey et al., 2018, Jia et al., 2021). Likelihood inference for PINAR and INAR models can be challenging; moreover, adding covariates to the models is non-trivial. See Joe (2019) for more in the stationary setting.

A different method for constructing seasonal count series uses a periodic renewal point processes as in Fralix et al. (2012) and Livsey et al. (2018). Here, a zero-one binary sequence $\{B_t\}_{t=1}^\infty$ is constructed to be periodically stationary and $\{B_{1,t}\}, \{B_{2,t}\}, \dots$ denote IID copies of $\{B_t\}_{t=1}^\infty$. The periodic count series is constructed via the superposition

$$X_t = \sum_{i=1}^{N_t} B_{i,t}.$$

Here, $\{N_t\}_{t=1}^\infty$ is a periodic IID sequence of count valued random variables independent of the $\{B_{i,t}\}$. For example, to obtain a correlated sequence $\{X_t\}$ with Poisson marginal distributions, $\{N_t\}$ is taken as independent Poisson in t ,

with N_{dT+v} having the mean $\lambda_\nu > 0$. Then it is easy to see that X_{dT+v} is Poisson distributed with mean $\lambda_\nu P(B_\nu = 1)$. Fralix et al. (2012), Lund and Livsey (2016), and Livsey et al. (2018) show how to produce the classical count marginal distributions (Poisson, binomial, and negative binomial) with this setup and consider $\{B_t\}$ processes constructed by clipping Gaussian processes.

While binary-based models typically have negative correlations whenever $\{B_t\}$ does, it can be difficult to achieve some marginal distributions. A prominent example of this is the often sought generalized Poisson marginal. Perhaps worse, likelihood methods of parameter inference appear intractable – current parameter inference methods use Gaussian pseudo-likelihoods, which only use the series' mean and covariance structure. See Davis et al. (2021) for additional detail.

Before proceeding, a clarification needs to be made. The models constructed here posit a particular count marginal distribution for the data *a priori*. This differs from dynamic linear modeling goals, where count models are often built from conditional specifications. For a time-homogeneous AR(1) example, a dynamic linear model might employ the state space setup $X_t | \alpha_t \sim \text{Poisson}(e^{\alpha_t})$, where $\alpha_t = \beta \alpha_{t-1} + \eta_t$, $|\beta| < 1$, and $\{\eta_t\}$ is zero mean Gaussian noise. Such a setup produces a conditional Poisson distribution, not a series with a Poisson marginal distribution. In fact, as Asmussen and Foss (2014) show, the marginal distribution in the above Poisson state space setup can be far from Poisson.

Additional work on periodic count series is contained in Moriña et al. (2011), Monteiro et al. (2015), Bentarzi and Bentarzi (2017), Aknouche et al. (2018), Santos et al. (2021), Aknouche et al. (2018), and Ouzzani and Bentarzi (2019). Most of these references take one of the above approaches. Motivated by Jia et al. (2021), this paper presents a different approach.

The rest of this paper proceeds as follows. The next section reviews periodic time series methods, focusing on periodic autoregressive moving-average (PARMA) and seasonal autoregressive moving-average (SARMA) difference equation structures. Section 3 clarifies our model and its properties. Section 4 narrates parameter estimation methods and Section 5 studies these techniques via simulation. Section 6 analyzes a twenty year segment of weekly rainy day counts in Seattle, Washington. Section 7 concludes with comments and remarks.

2 | PERIODIC TIME SERIES BACKGROUND

This section briefly reviews periodic (seasonal) time series. Our future count construction uses a series $\{Z_t\}$, standardized to $E[Z_t] \equiv 0$ and $\text{Var}(Z_t) \equiv 1$, and having Gaussian marginal distributions. While the mean of $\{Z_t\}$ is zero, periodic features in the autocorrelation function of $\{Z_t\}$, which we denote by $\rho_Z(t, s) = \text{Cov}(Z_t, Z_s)$, will become paramount.

We call $\{Z_t\}$ a PARMA(p, q) series if it obeys the periodic ARMA(p, q) difference equation

$$Z_{dT+v} = \sum_{k=1}^p \phi_k(\nu) Z_{dT+v-k} + \eta_{dT+v} + \sum_{k=1}^q \theta_k(\nu) \eta_{dT+v-k}. \quad (1)$$

Here, $\{\eta_t\}$ is a zero mean white noise sequence with the periodic variance $\text{Var}(\eta_{dT+v}) = \sigma^2(\nu) > 0$. The autoregressive order is p and the moving-average order is q , which are taken constant in the season ν for simplicity. The autoregressive and moving-average coefficients are $\phi_1(\nu), \dots, \phi_p(\nu)$ and $\theta_1(\nu), \dots, \theta_q(\nu)$, respectively, during season ν . We tacitly assume that model parameters are identifiable from the covariance of the series. This may require more than the classical causality and invertibility conditions (Reinsel, 2003). Gaussian PARMA solutions are strictly stationary with period T as long as the autoregressive polynomial does not have a root on the complex unit circle – see Lund and

Basawa (1999) for quantification. Not all PARMA parameters are free due to the restriction $\text{Var}(X_t) \equiv 1$; the following example delves further into the matter.

Example 3.1 A PAR(1) series with period T obeys the recursion

$$Z_t = \phi(t)Z_{t-1} + \eta_t, \quad (2)$$

where $\{\eta_t\}$ is zero mean white noise with $\text{Var}(\eta_t) = \sigma^2(t)$. The quantities $\phi(t)$ and $\sigma^2(t)$ are assumed periodic in t with period T . This difference equation is known to have a unique (in mean squared) and causal solution whenever there is a stochastic contraction over an entire cycle: $|\prod_{v=1}^T \phi(v)| < 1$ (Lund and Basawa, 1999).

To impose $\text{Var}(Z_t) \equiv 1$, take a variance on both sides of (2) and set $\text{Var}(Z_t) = \text{Var}(Z_{t-1}) = 1$ to infer that $\sigma^2(t) = 1 - \phi^2(t)$, which we tacitly assume is positive for all t . This uses $\text{Cov}(Z_{t-1}, \eta_t) = 0$, which follows by causality. The covariance structure of $\{Z_t\}$ can now be extracted as

$$\rho_Z(t, s) = \prod_{i=0}^{t-s-1} \phi(t-i).$$

for $s < t$. ♣.

Another class of periodic models in use today are the SARMA series. SARMA series are actually time-stationary models, but have comparatively large autocorrelations at lags that are multiples of the period T . The most basic SARMA(p, q) series $\{Z_t\}$ obeys a difference equation driven at lags that are multiples of the period T :

$$Z_t = \sum_{k=1}^p \phi_k Z_{t-kT} + \eta_t + \sum_{k=1}^q \theta_k \eta_{t-kT}, \quad (3)$$

where $\{\eta_t\}$ is zero mean independent noise with a constant variance. In this setup, $\rho_Z(t, s) = 0$ unless $t - s$ is a whole multiple of the period T . As such, many authors allow $\{\eta_t\}$ to have additional correlation, specifically a zero mean ARMA(p^*, q^*) series. This results in a model that can have non-zero correlations at any lag; however, the model is still stationary and does not have any true periodic features. Since the model is stationary, we write $\rho_Z(t, s) = \rho_Z(t - s)$.

Example 3.2 A SAR(1) series with period T and AR(1) $\{\eta_t\}$ obeys the difference equation pair

$$Z_t = \phi Z_{t-T} + \eta_t; \quad \eta_t = \alpha \eta_{t-1} + \epsilon_t, \quad (4)$$

where $\{\epsilon_t\}$ is zero mean white noise with variance σ_ϵ^2 , $|\phi| < 1$, and $|\alpha| < 1$. Combining these two difference equations results in a stationary and causal AR($T + 1$) model for $\{Z_t\}$.

Imposing $\text{Var}(Z_t) \equiv 1$ and taking a variance in the first equation in (4) gives

$$1 = \phi^2 + \text{Var}(\eta_t) + 2\phi \text{Cov}(Z_{t-T}, \eta_t).$$

To proceed, use equation (4)'s causal solutions $\eta_t = \sum_{k=0}^{\infty} \alpha^k \epsilon_{t-k}$ and $Z_{t-\ell} = \sum_{m=0}^{\infty} \phi^m \eta_{t-mT-\ell}$ to get

$$\text{Cov}(\eta_t, Z_{t-\ell}) = \sigma_\epsilon^2 \frac{\alpha^\ell}{(1 - \alpha^2)(1 - \phi\alpha^T)} \quad (5)$$

for any $\ell > 0$. Combining the last two equations, we see that taking

$$\sigma_e^2 = \frac{(1 - \phi^2)(1 - \alpha^2)(1 - \phi\alpha^T)}{1 + \phi\alpha^T} \quad (6)$$

indices $\text{Var}(Z_t) \equiv 1$.

To extract the covariance structure of $\{Z_t\}$, multiply both sides of (4) by Z_{t-h} and take expectations to get the Yule-Walker type equations

$$\begin{aligned} \rho_Z(0) &= \phi\rho_Z(T) + E(Z_t\eta_t) \\ &\vdots \\ \rho_Z(T) &= \phi\rho_Z(0) + E(Z_{t-T}\eta_t). \end{aligned}$$

This system can be rewritten in vector form as

$$\begin{bmatrix} 1 & 0 & \cdots & 0 & -\phi \\ 0 & 1 & \cdots & -\phi & 0 \\ \vdots & \vdots & \vdots & \vdots & \vdots \\ 0 & -\phi & \cdots & 1 & 0 \\ -\phi & 0 & \cdots & 0 & 1 \end{bmatrix} \begin{bmatrix} \rho_Z(0) \\ \rho_Z(1) \\ \vdots \\ \rho_Z(T-1) \\ \rho_Z(T) \end{bmatrix} = \begin{bmatrix} E(\eta_t Z_t) \\ E(\eta_t Z_{t-1}) \\ \vdots \\ E(\eta_t Z_{t-T+1}) \\ E(\eta_t Z_{t-T}) \end{bmatrix}.$$

One can show that the inverse of the matrix in the above linear system exists. From this, (5), (6), and some very tedious algebraic manipulations, one can extract

$$\rho_Z(h) = \frac{\alpha^h + \phi\alpha^{T-h}}{1 + \phi\alpha^T}, \quad 0 \leq h \leq T.$$

For the $h > T$ model correlations, multiply the first equation in (4) by Z_{t-h} for $h > T$ and take expectations to get the recursion $\rho_Z(h) = \phi\rho_Z(h-T) + E(\eta_t Z_{t-h})$. This can be solved with (5) to get

$$\rho_Z(h) = \phi^a \frac{\alpha^b + \phi\alpha^{T-b}}{1 + \phi\alpha^T} + \sum_{k=0}^{a-1} \phi^k \alpha^{h-Tk} \frac{1 - \alpha^2}{1 + \phi\alpha}, \quad h > T,$$

where $a = \lfloor h/T \rfloor$ and $b = h - aT$. ♣.

PARMA and SARMA methods are compared in detail in Lund (2011). PARMA models are usually more applicable since the immediate past of the process is typically more influential than past process lags at multiples of the period T . Applications in the environment (Vecchia, 1985, Bloomfield et al., 1994, Lund et al., 1995, Tesfaye et al., 2004) tend to be PARMA; SARMA structures are useful in economics (Franses, 1994, Franses and Paap, 2004, Hurd and Miamee, 2007). PARMA reviews are Gardner and Franks (1975), Lund and Basawa (1999), and Gardner et al. (2006); statistical inference for PARMA models is studied in Lund and Basawa (2000), Basawa and Lund (2001), Basawa et al. (2004), Lund et al. (2006), Shao and Ni (2004), and Shao (2006). SARMA inference is addressed in Chatfield and Prothero (1973).

3 | METHODOLOGY

Our methods extend the work in Jia et al. (2021) with Gaussian transformations (copulas) to the periodic setting. Let $\{X_t\}$ denote the time series to be constructed, which takes values in the count support set $\{0, 1, 2, \dots\}$. Our construction works with a latent Gaussian series $\{Z_t\}$ with zero mean and a unit variance at all times. Then X_t is obtained from Z_t via

$$X_{dT+\nu} = F_\nu^{-1}(\Phi(Z_{dT+\nu})), \quad (7)$$

where $\Phi(\cdot)$ is the cumulative distribution function (CDF) of the standard normal distribution and $F_\nu(\cdot)$ is the desired marginal distribution for X_t during season ν . Here, F_ν^{-1} is the quantile function

$$F_\nu^{-1}(u) = \inf \{x : F_\nu(x) \geq u\}. \quad (8)$$

As Jia et al. (2021) shows, this construction leaves $X_{dT+\nu}$ with the marginal distribution F_ν for every d and ν . This model is very flexible: any marginal distribution can be achieved for any desired season ν , even continuous ones. The marginal distribution F_ν can have the same form or be different for distinct seasons ν . Any marginal distribution whatsoever can be achieved; when count distributions are desired, the quantile definition in (8) is the version of the inverse CDF that produces the desired marginals.

3.1 | Properties of the Model

Toward ARMA and PARMA model order identification, if $\{Z_t\}$ is an m -dependent series, then Z_{t_1} and Z_{t_2} are independent when $|t_1 - t_2| > m$ since $\{Z_t\}$ is Gaussian. By (7), X_{t_1} and X_{t_2} are also independent and $\{X_t\}$ is also m -dependent. From the characterization of stationary moving averages (Proposition 3.2.1 in Brockwell and Davis (1991)) and periodic moving-averages in Shao and Lund (2004), we see that if $\{Z_t\}$ is a periodic moving average of order q , then $\{X_t\}$ is also a periodic moving average of order q . Unfortunately, analogous results for autoregressions do not hold. For example, if $\{Z_t\}$ is a periodic first order autoregression, $\{X_t\}$ may not be a periodic autoregression of any order (Jia et al., 2021).

We now derive the covariance structure of $\{X_t\}$ via Hermite expansions. Let $\gamma_X(t, r) = \text{Cov}(X_t, X_r)$ be the covariance of $\{X_t\}$ at times t and r , where $r \leq t$. Then $\gamma_X(t, r)$ can be related to $\rho_Z(t, r)$ via Hermite expansions. To do this, let $G_\nu(x) = F_\nu^{-1}(\Phi(x))$ and write the Hermite expansion of $G_\nu(\cdot)$ as

$$G_\nu(z) = g_0(\nu) + \sum_{k=1}^{\infty} g_k(\nu) H_k(z). \quad (9)$$

Here, $g_k(\nu)$ is the k th Hermite coefficient for season ν , whose calculation is described below, and $H_k(z)$ is the k th Hermite polynomial defined by

$$H_k(z) = (-1)^k e^{z^2/2} \frac{d^k}{dz^k} \left(e^{-z^2/2} \right). \quad (10)$$

The first three Hermite polynomials are $H_0(x) \equiv 1$, $H_1(x) = x$, and $H_2(x) = x^2 - 1$. Higher order polynomials can be found via the recursion $H_k(x) = xH_{k-1}(x) - H'_{k-1}(x)$, which follows from (10).

The polynomials H_k and H_j are orthogonal with respect to the standard Gaussian measure if $k \neq j$: $E[H_k(Z)H_j(Z)] = 0$ for a standard normal Z unless $j = k$ (in which case $E[H_k(Z)^2] = k!$). The Hermite coefficients are computed from

$$g_k(v) = \frac{1}{k!} \int_{-\infty}^{\infty} G_v(t) H_k(t) \phi(t) dt, \quad k = 1, 2, \dots, \quad (11)$$

where $\phi(t) = \Phi'(t) = e^{-t^2/2}/\sqrt{2\pi}$ is the standard normal density.

Lemma 2.1 in Han and De Oliveira (2016) shows that

$$\gamma_X(t, r) = \sum_{k=1}^{\infty} k! g_k(s(t)) g_k(s(r)) \rho_Z(t, r)^k, \quad (12)$$

where $s(t) = t - T \lfloor (t+1)/T \rfloor$ denotes the season corresponding to time t . Let $\sigma_X^2(t) = \gamma_X(t, t) = \sum_{k=1}^{\infty} k! g_k^2(s(t))$ denote the variance of X_t . Then the ACF of $\{X_t\}$ is

$$\rho_X(t, r) = \frac{\gamma_X(t, r)}{\sigma_X(t)\sigma_X(r)} = \sum_{k=1}^{\infty} \frac{k! g_k(s(t)) g_k(s(r))}{\sigma_X(t)\sigma_X(r)} \rho_Z(t, r)^k = \sum_{k=1}^{\infty} \ell_k \rho_Z(t, r)^k := L(\rho_Z(t, r)), \quad (13)$$

which is a power series in $\rho_Z(t, r)$ with k th coefficient

$$\ell_k := \frac{k! g_k(s(t)) g_k(s(r))}{\sigma_X(t)\sigma_X(r)}. \quad (14)$$

Jia et al. (2021) call $L(\cdot)$ a link function and ℓ_k a link coefficient. When $\{Z_t\}$ is stationary and F_ν does not depend on ν , they show that $L(0) = 0$, $L(1) = 1$, and $L(-1) = \text{Corr}(G(Z_0), G(-Z_0))$. It is not true that $L(-1) = -1$ in any case nor is $L(1) = 1$ in the periodic case; indeed, stationary or periodically stationary count processes with arbitrarily positive or negative correlations may not exist. For example, the pair $(Z, -Z)$, where Z is standard normal has correlation -1, but two Poisson random variables, both having mean λ , whose correlation is -1, do not exist.

The model produces the most flexible correlation structures possible in a pairwise sense. Specifically, consider two distinct seasons ν_1 and ν_2 and suppose that F_{ν_1} and F_{ν_2} are the corresponding marginal distributions for these seasons. Then Theorems 2.1 and 2.5 in Whitt (1976) show that the bivariate random pair (X_{ν_1}, X_{ν_2}) having the marginal distributions F_{ν_1} and F_{ν_2} , respectively, with the largest correlation has form $X_{\nu_1} = F_{\nu_1}^{-1}(U)$ and $X_{\nu_2} = F_{\nu_2}^{-1}(U)$, where U is a uniform[0,1] random variable. To achieve the largest correlation, one simply takes $\{Z_t\}$ to have unit correlation at these times; that is, take $Z_{\nu_1} = Z_{\nu_2}$. Since $\Phi(Z_{\nu_1})$ is uniform[0,1], the claim follows. For negative correlations, the same results in Whitt (1976) also show that the most negatively correlated pair that can be produced has the form $X_{\nu_1} = F_{\nu_1}^{-1}(U)$ and $X_{\nu_2} = F_{\nu_2}^{-1}(1-U)$. This is produced with a Gaussian series having $\text{Corr}(Z_{\nu_1}, Z_{\nu_2}) = -1$, which is obtained by selecting $Z_{\nu_2} = -Z_{\nu_1}$. Then $\Phi(Z_{\nu_1})$ is again uniform[0,1] and $\Phi(Z_{\nu_2}) = \Phi(-Z_{\nu_1}) = 1 - \Phi(Z_{\nu_1})$, since $\Phi(-x) = 1 - \Phi(x)$ for all real x .

The previous paragraph implies that one cannot construct more general autocorrelation functions for count series than what has been constructed above – they do not exist. Negatively correlated count series do arise (Kachour and Yao, 2009, Livsey et al., 2018, Jia et al., 2021) and can be described with this model class. In the stationary case where the marginal distribution F_ν is constant over all seasons ν , a series $\{X_t\}$ with $\text{Cov}(X_t, X_{t+h}) = 1$ for all h is achieved by taking $Z_t \equiv Z$, where Z is standard normal. This unit correlation property will not carry over to our periodic setting. For example, a random pair (X_{ν_1}, X_{ν_2}) having a Poisson marginal with mean λ_{ν_1} during season ν_1 and a Poisson marginal with mean λ_{ν_2} during season ν_2 with a unit correlation do not exist when $\lambda_{\nu_1} \neq \lambda_{\nu_2}$. This said, the

model can produce any correlation structures within "the range of achievable correlations". As such, the model class here is quite flexible.

The amount of autocorrelation that $\{X_t\}$ inherits from $\{Z_t\}$ is now discussed. An implication of the result below, which establishes monotonicity of the link function by showing that its derivative is positive, is that the larger the autocorrelations are in $\{Z_t\}$, the larger the autocorrelations are in $\{X_t\}$. We state the result below and prove it in the Appendix.

Proposition 3.1: *For a fixed t and r , let $L(\cdot)$ denote the link function in (13). Then for $u \in (-1, 1)$, the derivative of the link is positive and has form*

$$L'(u) = \frac{\sum_{j_1=0}^{\infty} \sum_{j_2=0}^{\infty} e^{-\frac{1}{2(1-u^2)}} \left[\Phi^{-1}(C_{j_1}(s(t)))^2 + \Phi^{-1}(C_{j_2}(s(r)))^2 - 2u \Phi^{-1}(C_{j_1}(s(t))) \Phi^{-1}(C_{j_2}(s(r))) \right]}{\sqrt{\sigma_X(t) \sigma_X(r)} 2\pi \sqrt{1-u^2}}. \quad (15)$$

Here,

$$C_j(v) = \mathbb{P}[X_v \leq j] \quad (16)$$

denotes the cumulative probabilities of X_v at season v .

3.2 | Calculation and Properties of the Hermite Coefficients

An important numerical task entails calculating $g_k(v)$, which only depends on $F_v(\cdot)$ by (11). To do this, rewrite $G_v(z)$ in the form

$$G_v(z) = \sum_{j=0}^{\infty} j \mathbb{1}_{[C_{j-1}(v) \leq \Phi^{-1}(z) < C_j(v)]} = \sum_{j=1}^{\infty} j \mathbb{1}_{[\Phi^{-1}(C_{j-1}(v)), \Phi^{-1}(C_j(v))]}(z), \quad (17)$$

where the convention $C_{-1} = 0$ is made. We also take $\Phi^{-1}(0) = -\infty$ and $\Phi^{-1}(1) = \infty$. Then for $k \geq 1$, integration by parts yields

$$\begin{aligned} g_k(v) &= \frac{1}{k!} \sum_{j=0}^{\infty} n \mathbb{E} \left[\mathbb{1}_{[\Phi^{-1}(C_{j-1}(v)), \Phi^{-1}(C_j(v))]}(Z_0) H_k(Z_0) \right] \\ &= \frac{1}{k!} \sum_{j=0}^{\infty} \frac{j}{\sqrt{2\pi}} \int_{\Phi^{-1}(C_{j-1}(v))}^{\Phi^{-1}(C_j(v))} H_k(z) e^{-z^2/2} dz \\ &= \frac{1}{k!} \sum_{j=0}^{\infty} \frac{j}{\sqrt{2\pi}} \int_{\Phi^{-1}(C_{j-1}(v))}^{\Phi^{-1}(C_j(v))} (-1)^k \left(\frac{d^k}{dz^k} e^{-z^2/2} \right) dz \\ &= \frac{1}{k!} \sum_{j=0}^{\infty} \frac{j}{\sqrt{2\pi}} (-1)^k \left(\frac{d^{k-1}}{dz^{k-1}} e^{-z^2/2} \right) \Big|_{z=\Phi^{-1}(C_{j-1}(v))}^{z=\Phi^{-1}(C_j(v))} \\ &= \frac{1}{k!} \sum_{j=0}^{\infty} \frac{j}{\sqrt{2\pi}} (-1)^k e^{-z^2/2} H_{k-1}(z) \Big|_{z=\Phi^{-1}(C_{j-1}(v))}^{z=\Phi^{-1}(C_j(v))}. \end{aligned}$$

Simplifying this telescoping sum gives

$$g_k(v) = \frac{1}{k! \sqrt{2\pi}} \sum_{j=0}^{\infty} e^{-[\Phi^{-1}(C_j(v))]^2/2} H_{k-1}(\Phi^{-1}(C_j(v))). \quad (18)$$

Notice that the summands in (18) are zero whenever $\Phi^{-1}(C_j(v)) = \pm\infty$. Lemma 2.1 in Jia et al. (2021) shows that the expansion converges whenever $\mathbb{E}[X_t^\rho] < \infty$ for some $\rho > 1$. This condition automatically holds for time series, which implicitly require a finite second moment. For count distributions with a finite support, $C_j(v)$ becomes unity for large j . For example, a Binomial marginal distribution with 7 trials is considered in our later application. Here, the summation can be reduced to $j \in \{0, 1, \dots, 7\}$. For count distributions on a countably infinite support, approximating (18) requires truncation of an infinite series. This is usually not an issue: numerically, $C_j(v)$ quickly converges to unity as $j \rightarrow \infty$ for light tailed distributions – or equivalently, $e^{-\Phi^{-1}(C_j(v))^2/2} H_{k-1}(\Phi^{-1}(C_j(v))) \rightarrow 0$. In addition to (18), $g_k(v)$ can also be approximated by Gaussian quadrature; see *gauss.quad.prob* in the package *statmod* in R. However, the approximation in (18) is more appealing in terms of simplicity and stability (Jia et al., 2021).

4 | PARAMETER INFERENCE

This section develops likelihood methods of inference for the model parameters via particle filtering and sequential Monte Carlo techniques. With many count time series model classes, likelihoods are intractable (Davis et al., 2021). Accordingly, researchers have defaulted to moment and composite likelihood techniques. However, if the count distributional structure truly matters, likelihood methods should “feel” this structure and return superior parameter estimates. Gaussian pseudo-likelihood estimates, which are based only on the mean and autocovariance of the series, are developed in Jia et al. (2021) in the stationary case. Jia et al. (2021) presents an example where Gaussian pseudo-likelihood estimates perform well and an example where they perform poorly.

For notation, let θ contain all parameters in the T marginal distributions F_1, \dots, F_T and η contain all parameters governing the evolution of $\{Z_t\}$. The data $\{x_1, x_2, \dots, x_n\}$ denote our realization of the series.

The likelihood function $\mathcal{L}(\theta, \eta)$ is simply a high dimensional multivariate normal probability. To see this, use (7) to get

$$\mathcal{L}(\theta, \eta) = \mathbb{P}(X_1 = x_1, \dots, X_n = x_n) = \mathbb{P}(Z_1 \in (a_1, b_1], \dots, Z_n \in (a_n, b_n]) \quad (19)$$

for some numbers $\{a_i\}_{i=1}^n$ and $\{b_i\}_{i=1}^n$ (these are clarified below but are not important here). The covariance matrix of (Z_1, \dots, Z_n) only depends on η , not on θ . Unfortunately, evaluating a high dimensional multivariate normal probability is numerically challenging for large n . While methods to handle this problem exist (Kazianka and Pilz, 2010, Kazianka, 2013, Bai et al., 2014), they often contain substantial estimation bias.

An alternative approach, which is the one taken here, uses simulation methods to approximate the likelihood. General methods in this category include the quasi-Monte Carlo methods of Genz and Bretz (2002) and the prominent Geweke–Hajivassiliou–Keane (GHK) simulator of Geweke (1991) and Hajivassiliou et al. (1996). The performance of these methods, along with an additional “data cloning” approach, are compared in Han and De Oliveira (2020), where the author shows that estimators from these methods are similar, but that the GHK methods are much faster, having a numerical complexity as low as order mn . Here, m is the pre-selected number of sample paths to be simulated (the number of particles). As we will subsequently see, the GHK simulator works quite well for large m .

Jia et al. (2021) propose a sequential importance sampling method that uses a modified GHK simulator. In essence,

importance sampling is used to evaluate integrals by drawing samples from an alternative distribution and averaging their corresponding weights. Suppose that we seek to estimate $\int_{\mathcal{D}} f(\mathbf{x}) d\mathbf{x}$. Then

$$\int_{\mathcal{D}} f(\mathbf{x}) d\mathbf{x} = \int_{\mathcal{D}} \frac{f(\mathbf{x})}{q(\mathbf{x})} q(\mathbf{x}) d\mathbf{x},$$

where $f(\mathbf{x})/q(\mathbf{x})$ is called the weight and the proposed distribution q is called the importance distribution. Without loss of generality, we assume that $q(\mathbf{x}) > 0$ whenever $\mathbf{x} \in \mathcal{D}$ and that $q(\mathbf{x}) = 0$ for $\mathbf{x} \in \mathcal{D}^c$. Then the importance sampling estimate of the integral is the law of large numbers justified average

$$\int_{\mathcal{D}} \frac{f(\mathbf{x})}{q(\mathbf{x})} q(\mathbf{x}) d\mathbf{x} \approx \frac{1}{m} \sum_{k=1}^m \frac{f(\mathbf{x}^{(k)})}{q(\mathbf{x}^{(k)})},$$

where $\{\mathbf{x}^{(1)}, \dots, \mathbf{x}^{(m)}\}$ are m IID samples drawn from the proposed distribution q . With the notation $\mathbf{z}_{1:n} = (z_1, \dots, z_n)$, notice that the likelihood in (19) has form

$$\int_{\{z_t \in (a_t, b_t], t=1, \dots, n\}} \phi_{\eta}(\mathbf{z}_{1:n}) dz_1 \dots dz_n = \int_{\{z_t \in (a_t, b_t], t=1, \dots, n\}} \frac{\phi_{\eta}(\mathbf{z}_{1:n})}{q(\mathbf{z}_{1:n})} q(\mathbf{z}_{1:n}) dz_1 \dots dz_n. \quad (20)$$

Observe that $\{a_i\}_{i=1}^n$ and $\{b_i\}_{i=1}^n$ only depend on θ and the data $\{x_1, x_2, \dots, x_n\}$. Specifically,

$$a_t = \Phi^{-1}(C_{x_{t-1}}(s(t))) \quad \text{and} \quad b_t = \Phi^{-1}(C_{x_t}(s(t))),$$

where $C_n(v)$ is defined in (16) and $s(t)$ is the season at time t . Here, it is best to choose a proposed distribution q such that 1) $q(\mathbf{z}_{1:n}) > 0$ for $z_t \in (a_t, b_t]$ and $q(\mathbf{z}_{1:n}) = 0$ otherwise; 2) the weight $\phi_{\eta}(\mathbf{z}_{1:n})/q(\mathbf{z}_{1:n})$ is easy to compute; and 3) $\{Z_t\}$ can be efficiently drawn from q . Our GHK simulator satisfies all three conditions.

To develop our GHK sampler further, we take advantage of the latent Gaussian structure in the PARMA or SARMA series $\{Z_t\}$. In simple cases, $\{Z_t\}$ may even be a Markov chain. The GHK algorithm samples Z_t , depending on the its previous history Z_{t-1}, \dots, Z_1 and X_t , from a truncated normal density. Specifically, let $\rho_{\eta(t)}(z_t | z_{t-1}, \dots, z_1, x_t)$ denote the truncated normal density of Z_t given the history Z_{t-1}, \dots, Z_1 and $X_t = x_t$. Then

$$\rho_{\eta(t)}(z_t | z_{t-1}, \dots, z_1, x_t) = \frac{1}{r_t} \left[\frac{\phi\left(\frac{z_t - \hat{z}_t}{r_t}\right)}{\Phi\left(\frac{b_t - \hat{z}_t}{r_t}\right) - \Phi\left(\frac{a_t - \hat{z}_t}{r_t}\right)} \right], \quad a_t < z_t < b_t, \quad (21)$$

where \hat{z}_t and r_t are the one-step-ahead mean and standard deviation of Z_t conditioned on z_1, z_2, \dots, z_n . Again, a_t and b_t only depend on x_t . Here, we choose the importance sampling distribution

$$q_{\eta}(\mathbf{z}_{1:n} | x_{1:n}) = \rho_{\eta(1)}(z_1 | x_1) \prod_{t=2}^n \rho_{\eta(t)}(z_t | z_{t-1}, \dots, z_1, x_t). \quad (22)$$

Elaborating further, let $\mathcal{N}(\mu, \sigma^2; a, b)$ denote a normal random variable with mean μ , σ^2 and variance σ^2 that is known to lie in (a, b) , where $a < b$. Then X_1 is first drawn from $\mathcal{N}(0, 1; a_1, b_1)$. Thereafter, X_2, X_3, \dots, X_n are sequentially sampled from the distribution in (21). The proposed importance sampling distribution is efficient to sample, has the

desired distributional support, and induces an explicit expression for the weights:

$$\frac{\phi_{\eta(t)}(z_{1:n})}{q_{\eta(t)}(z_{1:n}|x_{1:n})} = \frac{p_{\eta(1)}(z_1)}{p_{\eta(1)}(z_1|x_1)} \prod_{t=2}^n \frac{p_{\eta(t)}(z_t|z_{t-1}, \dots, z_1)}{p_{\eta(t)}(z_t|z_{t-1}, \dots, z_1, x_t)}.$$

Using (21) gives

$$\frac{p_{\eta}(z_t|z_{t-1}, \dots, z_1)}{p_{\eta}(z_t|z_{t-1}, \dots, z_1, x_t)} = \Phi\left(\frac{b_t - \hat{z}_t}{r_t}\right) - \Phi\left(\frac{a_t - \hat{z}_t}{r_t}\right).$$

Therefore,

$$\frac{\phi_{\eta}(z_{1:n})}{q(z_{1:n})} = [\Phi(b_1) - \Phi(a_1)] \prod_{t=2}^n \left[\Phi\left(\frac{b_t - \hat{z}_t}{r_t}\right) - \Phi\left(\frac{a_t - \hat{z}_t}{r_t}\right) \right].$$

Define the initial weight $w_1 = \Phi(b_1) - \Phi(a_1)$. We then recursively update the weights via

$$w_t = w_{t-1} \left[\Phi\left(\frac{b_t - \hat{z}_t}{r_t}\right) - \Phi\left(\frac{a_t - \hat{z}_t}{r_t}\right) \right]$$

at time t during the sequential sampling procedure. At the end of the sampling, we obtain

$$w_n = \frac{\phi_{\eta}(z_{1:n})}{q_{\eta}(z_{1:n}|x_{1:n})}.$$

In the classic GHK simulator, \hat{Z}_t and r_t^2 are obtained from a Cholesky decomposition of the covariance matrix of $\{Z_t\}$. Here, they are based on the PARMA or SARMA model for $\{Z_t\}$.

The full sequential importance sampling procedure is summarized below.

- 1 Initialize the process by sampling Z_1 from the $\mathcal{N}(0, 1; C_{x_1}(s(1)), C_{x_1}(s(1)))$ distribution. Define the weight w_1 by

$$w_1 = \Phi^{-1}(C_{x_1}(s(1))) - \Phi^{-1}(C_{x_{1-1}}(s(1))) \quad (23)$$

- 2 Now iterate steps 2 and 3 over $t = 2, 3, \dots, n$. Conditioned on Z_1, \dots, Z_{t-1} , generate

$$Z_t \stackrel{\mathcal{D}}{=} \mathcal{N}\left(\hat{z}_t, r_t; \Phi^{-1}(C_{x_t}(s(t))), \Phi^{-1}(C_{x_{t-1}}(s(t)))\right). \quad (24)$$

For example, in the PAR(1) model, $\hat{Z}_t = \phi(t)Z_{t-1}$ for $t \geq 1$, with the startup condition $\hat{Z}_1 = 0$; $r_t = 1 - \phi^2(t)$ for $t > 1$ with the startup $r_1 = 1$.

- 3 Define the weight w_t via

$$w_t = w_{t-1} \left[\Phi\left(\frac{\Phi^{-1}(C_{x_t}(s(t))) - \hat{z}_t}{r_t}\right) - \Phi\left(\frac{\Phi^{-1}(C_{x_{t-1}}(s(t))) - \hat{z}_t}{r_t}\right) \right] \quad (25)$$

The above generates a fair draw of a single "particle path" $\{Z_t\}$ with the property that the $\{X_t\}$ series generated

from $\{Z_t\}$ yields the observations x_1, \dots, x_n . Repeating this process m independent times gives m simulated process trajectories. Let $\{Z^{(1)}, \dots, Z^{(m)}\}$ be these trajectories and denote their corresponding weights at time n by $\{w_n^{(k)}\}_{k=1}^m$.

The importance sampling estimate is given by

$$\hat{\mathcal{L}}^{\text{GHK}}(\theta, \eta) = \frac{1}{m} \sum_{k=1}^m w_n^{(k)}.$$

A large m provides more accurate estimation.

The popular "L-BGSF-B" gradient step and search method is used to optimize the estimated likelihood $\hat{\mathcal{L}}^{\text{GHK}}(\theta, \eta)$; other optimizers may also work. However, $\hat{\mathcal{L}}^{\text{GHK}}(\theta, \eta)$ is "noisy" due to the sampling. One popular fix to this smooths the estimated likelihood by generating a set of random quantities in the particle filtering through transformation and keeps them constant across the computations for different sets of parameters. This method, called common random numbers (CRNs), makes the simulated likelihood $\hat{\mathcal{L}}^{\text{GHK}}(\theta, \eta)$ relatively smooth in its parameters; see Kleinman et al. (1999) and Glasserman and Yao (1992) for more on CRNs. In practice, the CRN point estimator behaves similarly to those for regular likelihoods; moreover, the Hessian-based covariance matrix, which is based on the derivative of $\hat{\mathcal{L}}^{\text{GHK}}(\theta, \eta)$, behaves much better numerically when CRNs are used. As the next section demonstrates, this procedure will yield standard errors that are very realistic.

Turning to model diagnostics, the probability integral transform (PIT) is used as a tool to evaluate model fitness. PIT methods, proposed in Dawid (1984), check the statistical consistency between probabilistic forecasts and the observations. Under the ideal scenario that the observations are drawn from the prediction distribution and the predictive distribution is continuous, PIT residuals are uniformly distributed over $[0, 1]$. PIT histograms tend to be U -shaped when the observations are over-dispersed. Unfortunately, the above themes do not hold for discrete count data. To remedy this, Czado et al. (2009) propose a nonrandomized PIT residual where uniformity still holds. Quantifying this, write the conditional cumulative distribution function of X_t as

$$P_t(y) := \mathbb{P}(X_t \leq y | X_1 = x_1, \dots, X_{t-1} = x_{t-1}), y \in \{0, 1, \dots\}. \quad (26)$$

Then the nonrandomized mean PIT residual is defined as $\bar{F}(u) = n^{-1} \sum_{t=1}^n F_t(u|x_t)$, where

$$F_t(u|y) = \begin{cases} 0, & \text{if } u \leq P_t(y-1) \\ \frac{u - P_t(y-1)}{P_t(y) - P_t(y-1)}, & \text{if } P_t(y-1) < u < P_t(y) \\ 1, & \text{if } u \geq P_t(y) \end{cases}. \quad (27)$$

The quantity $P_t(y)$ can be approximated during the particle filtering algorithms; specifically,

$$\hat{P}_t(y) = \sum_{i=0}^y w_{i,t}(\hat{Z}_t), \quad (28)$$

where

$$w_{i,t}(z) = \Phi\left(\frac{\Phi^{-1}(C_i(s(t))) - z}{r_t}\right) - \Phi\left(\frac{\Phi^{-1}(C_{i-1}(s(t))) - z}{r_t}\right).$$

The weight $w_{i,t}(z)$ can be obtained at time t during the particle filtering algorithm.

5 | SIMULATIONS

This section presents a simulation study to evaluate the performance of our estimation methods. Periodic time series models often have a large number of parameters. One way of consolidating these parameters into a parsimonious tally involves placing Fourier parametric constraints on the model parameters (Lund et al., 2006, Anderson et al., 2007), as is done below.

5.1 | Poisson Marginals

Our first simulation examines the classical Poisson count distribution with the PAR(1) $\{Z_t\}$ in Example 2.1. Here, F_ν is taken as a Poisson marginal with mean $\lambda(\nu)$, where the first-order Fourier constraint

$$\lambda(\nu) = a_1 + a_2 \cos\left(\frac{2\pi(\nu - a_3)}{T}\right)$$

is imposed to consolidate the T mean parameters into three. Here, $|a_2| < a_1$ is imposed to keep $\lambda(\nu)$ non-negative. The periods $T = 10$ and $T = 50$ are studied, the latter taken to roughly correspond to our future application to weekly rainy day counts. Our $\{Z_t\}$ process obeys

$$Z_t = \phi(t)Z_{t-1} + \varepsilon_t \sqrt{1 - \phi(t)^2},$$

with the AR coefficient $\phi(\nu)$ also being constrained by a first-order Fourier series that induces a causal model:

$$\phi(\nu) = b_1 + b_2 \cos\left(\frac{2\pi(\nu - b_3)}{T}\right). \quad (29)$$

These specifications ensure that $\{Z_t\}$ is a standard normal process ($E[Z_t] \equiv 0$ and $\text{Var}(Z_t) \equiv 1$). The parameters chosen must be legitimate in that $\lambda(\nu)$ must be positive for each ν and the PAR(1) model must be causal. A six-parameter scheme that obeys these constraints is $a_1 = 10$, $a_2 = 5$, $a_3 = 5$; $b_1 = 0.5$, $b_2 = 0.2$, and $b_3 = 5$, which is now studied.

For each MLE optimization, $m = 500$ independent particles are used along with series lengths of $n = 100$ and $n = 300$. CRN techniques are used to ensure that the likelihood is relatively smooth with respect to its parameters. This is an essential step – see Masarotto et al. (2017), Han and De Oliveira (2018) for more on CRNs. Identifiability issues with the phase shift Fourier parametrizations arise since $a \cos(\pi/2 - b) = -a \cos(b - \pi/2)$; because of this, we impose $a_3, b_3 \in [0, T)$. Finally, The popular quasi-Newton method L-BFGS-B is implemented to optimize the likelihoods (Steenbergen, 2006).

Figure 1 shows boxplots of parameter estimators aggregated from 500 independent series of various lengths and periods. The sample means of the parameter estimators are all close to their true values. When $T = 50$ and $n = 100$, there are only two complete cycles of data to estimate parameters from. For standard errors of these parameters, Table 1 reports two values: 1) sample standard deviations of the parameter estimators over the 500 runs (denominator of 499), and 2) the average (over the 500 runs) of standard errors obtained by inverting the Hessian matrix at the maximum likelihood estimate for each run (denominator of 500). Additional simulations (not shown here) with larger sample sizes with $T = 50$ show that any biases recede as n increases.

We next consider the same Poisson marginal case, but now change $\{Z_t\}$ to the SAR(1) series in Example 2.2. The a_1 , a_2 , and a_3 chosen for this simulation are the same as above. The SAR(1) parameters chosen are $\phi = 0.5$ and $\alpha = 0.3$.

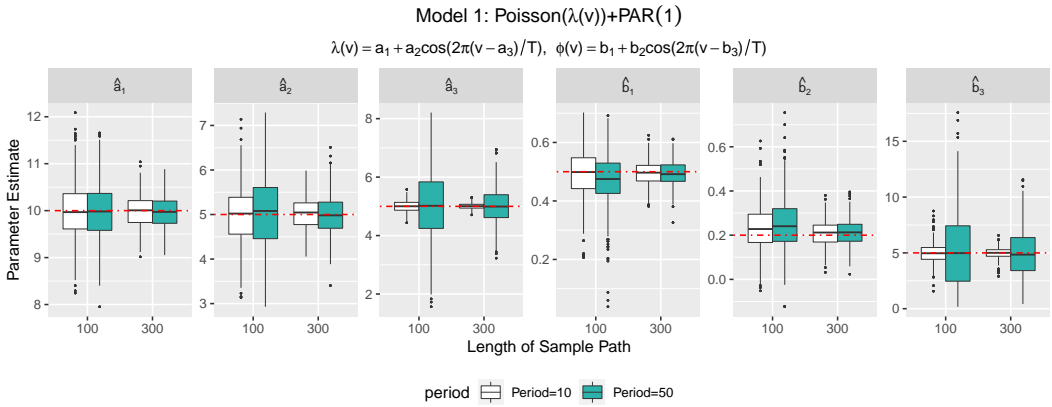


FIGURE 1 Box plots of parameter estimators for a Poisson marginal distribution with a PAR(1) $\{Z_t\}$. All estimators appear approximately unbiased – the dashed lines demarcate true parameter values.

Model 1								
n	T		\hat{a}_1	\hat{a}_2	\hat{a}_3	\hat{b}_1	\hat{b}_2	\hat{b}_3
100	10	mean	9.98375	5.00087	5.00443	0.49213	0.23474	4.98639
		SD	0.60068	0.63494	0.18490	0.07818	0.09896	0.90434
		$\hat{E}(I'(\theta)^2)$	0.57199	0.60025	0.17375	0.07720	0.10282	0.90060
100	50	mean	9.98127	5.05051	5.01370	0.46899	0.25285	5.24743
		SD	0.58975	0.79520	1.14622	0.08861	0.11470	3.50616
		$\hat{E}(I'(\theta)^2)$	0.59190	0.76871	1.11326	0.08268	0.11469	4.51175
300	10	mean	9.98652	5.01761	5.00714	0.49608	0.20812	4.98741
		SD	0.33694	0.36520	0.10039	0.04173	0.05550	0.48356
		$\hat{E}(I'(\theta)^2)$	0.32824	0.35012	0.09958	0.04151	0.05569	0.45228
300	50	mean	9.97370	4.98609	5.00089	0.49386	0.20998	4.89220
		SD	0.33449	0.45038	0.62028	0.04188	0.05726	2.09052
		$\hat{E}(I'(\theta)^2)$	0.34588	0.45153	0.65046	0.04156	0.05584	2.33228

TABLE 1 Standard errors for the parameter estimators for a Poisson marginal distribution with a PAR(1) $\{Z_t\}$. The results show the sample standard deviation (SD) of the parameter estimators from 500 independent series, and the average of the 500 standard errors obtained by inverting the Hessian matrix ($\hat{E}(I'(\theta)^2)$) at the maximum likelihood estimate over these same runs.

Figure 2 shows boxplots of the parameter estimators akin to those in Figure 1. The overall performance is again very good – interpretations of the results are similar to those for the PAR(1) model above. Table 2 shows our two types of standard errors and again reveals nice agreement.

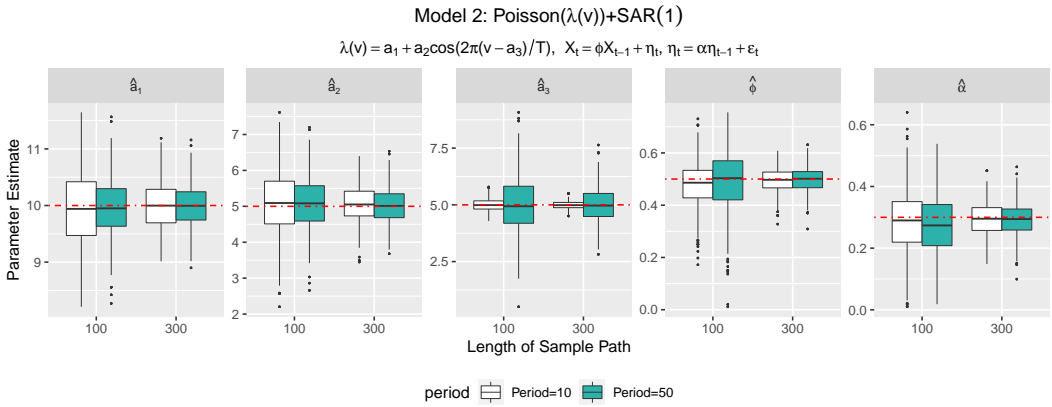


FIGURE 2 Box plots of parameter estimators for the Poisson marginal distribution with a SAR(1) $\{Z_t\}$. All estimators appear approximately unbiased – the dashed lines demarcate true parameter values.

Model 2							
n	T		\hat{a}_1	\hat{a}_2	\hat{a}_3	ϕ	α
		mean	9.94650	5.07987	4.99206	0.47876	0.28482
100	10	SD	0.66096	0.87087	0.26175	0.08455	0.10242
		$\hat{E}(I'(\theta)^2)$	0.65459	0.80021	0.25874	0.08242	0.09947
		mean	9.96430	5.07165	4.99623	0.49003	0.27121
100	50	SD	0.51019	0.71742	1.16749	0.11527	0.09630
		$\hat{E}(I'(\theta)^2)$	0.50809	0.68786	1.10774	0.10345	0.09874
		mean	9.99120	5.06420	4.99278	0.49535	0.29260
300	10	SD	0.41347	0.50127	0.15764	0.04399	0.05155
		$\hat{E}(I'(\theta)^2)$	0.40803	0.50201	0.15827	0.04269	0.05426
		mean	9.99133	5.01493	5.01603	0.49874	0.29189
300	50	SD	0.37005	0.49076	0.78444	0.04674	0.05392
		$\hat{E}(I'(\theta)^2)$	0.36755	0.49687	0.79666	0.04543	0.05403

TABLE 2 Standard errors for the parameter estimators for the Poisson marginal distribution with a SAR(1) $\{Z_t\}$. The results show the sample standard deviation (SD) of the parameter estimators from 500 independent series, and the average of the 500 standard errors obtained by inverting the Hessian matrix ($\hat{E}(I'(\theta)^2)$) at the maximum likelihood estimate over these same runs.

5.2 | A Markov Chain Induced Marginal Distribution

Another marginal distribution that we consider is derived from a two-state Markov chain (TSMC) model. This distribution will fit our weekly rainy day counts well in the next section. Consider a Markov transition matrix \mathbf{Q} on two states with form

$$\mathbf{Q} = \begin{bmatrix} \alpha & 1 - \alpha \\ 1 - \beta & \beta \end{bmatrix}.$$

Here, $\alpha \in (0, 1)$ is interpreted as the probability that day $t + 1$ is dry given that day t is dry; analogously, $\beta \in (0, 1)$ is the probability that day $t + 1$ is rainy given that day t is rainy. Let $\{M_t\}_{t=0}^7$ be a Markov chain with these transition probabilities. The marginal distribution that we consider for $\{X_t\}$ has the form

$$\mathbb{P}(X_t = k) = \mathbb{P}_{M_0} \left(\sum_{t=1}^7 M_t = k \right), \quad k \in \{0, 1, 2, 3, 4, 5, 6, 7\},$$

where $M_0 \in \{0, 1\}$. Here, $M_0 = 0$ signifies that the day before the week started was dry and $M_0 = 1$ signifies that the day before the week started was rainy. This marginal distribution, while difficult to derive in explicit form, allows for dependence in the day-to-day rain values, improving on a Binomial model with seven trials that models successive days as independent.

It is not easy to derive an explicit form for the distribution of F ; however, it can be built up numerically by allowing the number of days in a week to be a variable L and recursing on it:

$$\mathbb{P}_0 \left(\sum_{t=1}^L M_t = k \right) = (1 - \alpha) \mathbb{P}_1 \left(\sum_{t=1}^{L-1} M_t = k - 1 \right) + \alpha \mathbb{P}_0 \left(\sum_{t=1}^{L-1} M_t = k \right); \quad (30)$$

$$\mathbb{P}_1 \left(\sum_{t=1}^L M_t = k \right) = \beta \mathbb{P}_1 \left(\sum_{t=1}^{L-1} M_t = k - 1 \right) + (1 - \beta) \mathbb{P}_0 \left(\sum_{t=1}^{L-1} M_t = k \right). \quad (31)$$

These recursions start with probabilities for a one day week: $\mathbb{P}_0(M_t = 1) = 1 - \alpha$; $\mathbb{P}_0(M_t = 0) = \alpha$; $\mathbb{P}_1(M_t = 1) = \beta$, and $\mathbb{P}_1(M_t = 0) = 1 - \beta$. We take the initial state of the chain to be random with the stationary distribution

$$\mathbb{P}(M_0 = 0) = \frac{1 - \alpha}{2 - \alpha - \beta}; \quad \mathbb{P}(M_0 = 1) = \frac{1 - \beta}{2 - \alpha - \beta}.$$

To allow for periodicities in the above TSMC structure, we parametrize α and β as short Fourier series again:

$$\alpha(v) = a_1 + a_2 \cos \left(\frac{2\pi(v - a_3)}{T} \right); \quad \beta(v) = b_1 + b_2 \cos \left(\frac{2\pi(v - b_3)}{T} \right).$$

Our first TSMC simulation considers the PAR(1) $\{Z_t\}$ in (29). This is a nine parameter model. The parameter values considered are $a_1 = 0.4$, $a_2 = 0.2$, $a_3 = 5$; $b_1 = 0.5$, $b_2 = 0.2$, $b_3 = 0.3$, $c_1 = 0.2$, $c_2 = 0.1$, and $c_3 = 5$, which induce a causal $\{Z_t\}$ and legitimate Markov chain transitions (all transitions have non-negative probabilities). Figure 3 shows boxplots of the estimated parameters over 500 independent series of various lengths and periods. Table 3 shows standard errors computed from the two methods previously described. For the most part, the results are satisfying. Some of the phase shift parameter's "Hessian inverted" standard errors are larger than the sample standard deviation standard errors. The phase shift parameter is the argument where its associated cosine wave is maximal and lies

in $[0, T]$. Because of the larger support set, this parameter will naturally have more variability than say parameters supported in $(-1,1)$. Also, when $n = 100$ and $T = 50$, there are only two complete cycles from which to estimate the location of this maximum – this will be statistically difficult. Additional simulations (not reported) show that these discrepancies recede as the sample size gets larger.

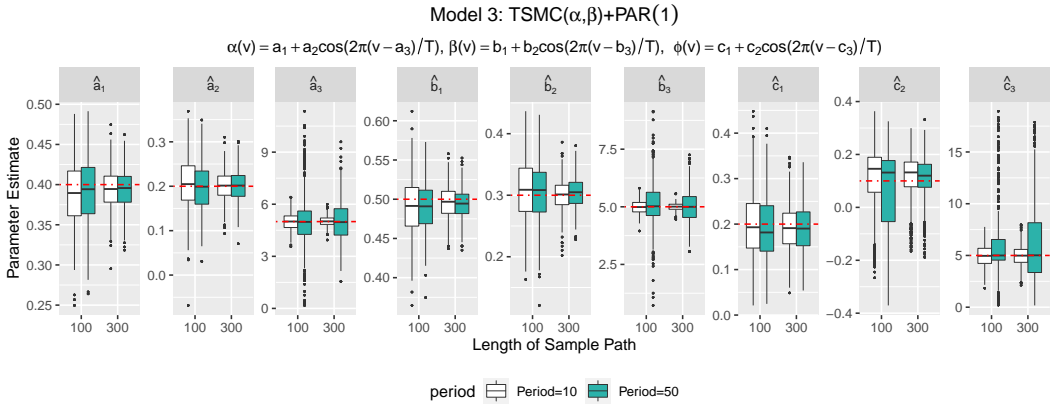


FIGURE 3 Box plots of parameter estimators for the TSMC marginal distribution with a PAR(1) $\{Z_t\}$. All estimators appear approximately unbiased – the dashed lines demarcate true parameter values.

Model 3											
n	T		\hat{a}_1	\hat{a}_2	\hat{a}_3	\hat{b}_1	\hat{b}_2	\hat{b}_3	\hat{c}_1	\hat{c}_2	\hat{c}_3
		mean	0.389	0.205	4.997	0.490	0.307	4.985	0.199	0.105	4.963
100	10	SD	0.041	0.060	0.472	0.036	0.048	0.295	0.076	0.134	1.221
		$\hat{E}(I'(\theta)^2)$	0.043	0.059	0.550	0.035	0.045	0.280	0.108	0.178	2.275
		mean	0.391	0.199	5.009	0.490	0.302	5.109	0.192	0.072	5.994
100	50	SD	0.040	0.057	1.876	0.032	0.050	1.137	0.072	0.153	4.153
		$\hat{E}(I'(\theta)^2)$	0.044	0.065	3.210	0.036	0.049	1.603	0.112	0.195	14.718
		mean	0.394	0.200	5.013	0.496	0.301	5.002	0.194	0.114	4.969
300	10	SD	0.024	0.033	0.306	0.021	0.026	0.159	0.052	0.084	1.095
		$\hat{E}(I'(\theta)^2)$	0.025	0.033	0.291	0.020	0.026	0.159	0.060	0.087	1.376
		mean	0.395	0.201	4.989	0.495	0.304	5.017	0.191	0.108	5.989
300	50	SD	0.024	0.035	1.269	0.020	0.026	0.733	0.053	0.085	4.130
		$\hat{E}(I'(\theta)^2)$	0.025	0.034	1.506	0.020	0.027	0.823	0.060	0.097	8.054

TABLE 3 Standard errors for the parameter estimators for the TSMC marginal distribution with a PAR(1) $\{Z_t\}$. The results show the sample standard deviation (SD) of the parameter estimators from 500 independent series, and the average of the 500 standard errors obtained by inverting the Hessian matrix $\hat{E}(I'(\theta)^2)$ at the maximum likelihood estimate over these same runs.

Finally, we consider the TSMC marginal distribution with a SAR(1) $\{Z_t\}$. Figure 4 shows boxplots of the estimated parameters over 500 independent series of various lengths and periods. Table 4 shows standard errors computed by our two methods. Again, the performance is good – the interpretation of the results is analogous to that given before.

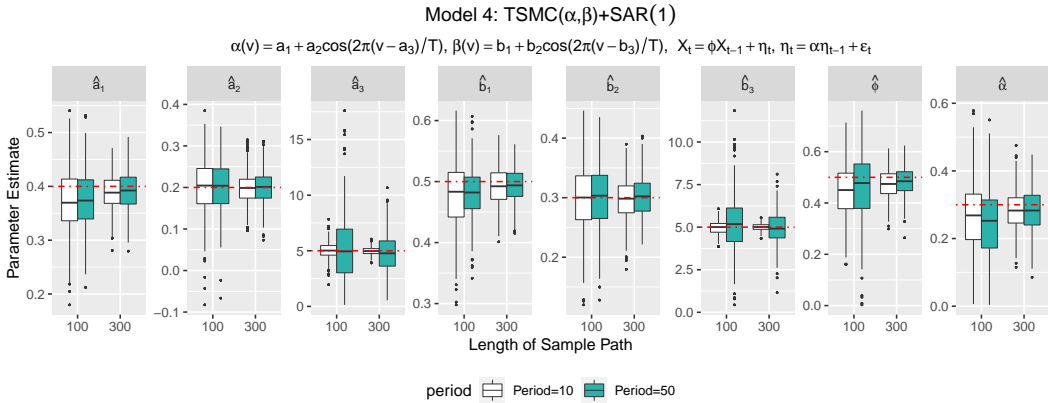


FIGURE 4 Box plots of parameter estimators for the TSMC marginal distribution with a SAR(1) $\{Z_t\}$. All estimators appear approximately unbiased – the dashed lines demarcate true parameter values.

Model 4										
n	T		\hat{a}_1	\hat{a}_2	\hat{a}_3	\hat{b}_1	\hat{b}_2	\hat{b}_3	ϕ	α
100	10	mean	0.372	0.200	4.995	0.480	0.299	5.010	0.447	0.260
		SD	0.061	0.068	0.605	0.050	0.056	0.356	0.107	0.111
		$\hat{E}(I'(\theta)^2)$	0.055	0.063	0.624	0.046	0.053	0.335	0.102	0.109
100	50	mean	0.378	0.199	4.890	0.482	0.299	5.106	0.469	0.250
		SD	0.049	0.060	2.807	0.044	0.048	1.564	0.123	0.104
		$\hat{E}(I'(\theta)^2)$	0.049	0.062	3.602	0.040	0.050	1.572	0.121	0.107
300	10	mean	0.388	0.201	5.006	0.493	0.302	5.004	0.477	0.289
		SD	0.033	0.038	0.317	0.030	0.032	0.202	0.056	0.063
		$\hat{E}(I'(\theta)^2)$	0.033	0.038	0.335	0.028	0.032	0.193	0.054	0.060
300	50	mean	0.390	0.199	5.030	0.492	0.302	5.016	0.483	0.281
		SD	0.033	0.040	1.689	0.027	0.031	1.061	0.055	0.059
		$\hat{E}(I'(\theta)^2)$	0.032	0.038	1.706	0.027	0.032	0.960	0.056	0.060

TABLE 4 Standard errors for the parameter estimators for the TSMC marginal distribution with a SAR(1) $\{Z_t\}$. The results show the sample standard deviation (SD) of the parameter estimators from 500 independent series, and the average of the 500 standard errors obtained by inverting the Hessian matrix $(\hat{E}(I'(\theta)^2))$ at the maximum likelihood estimate over these same runs.

6 | APPLICATION

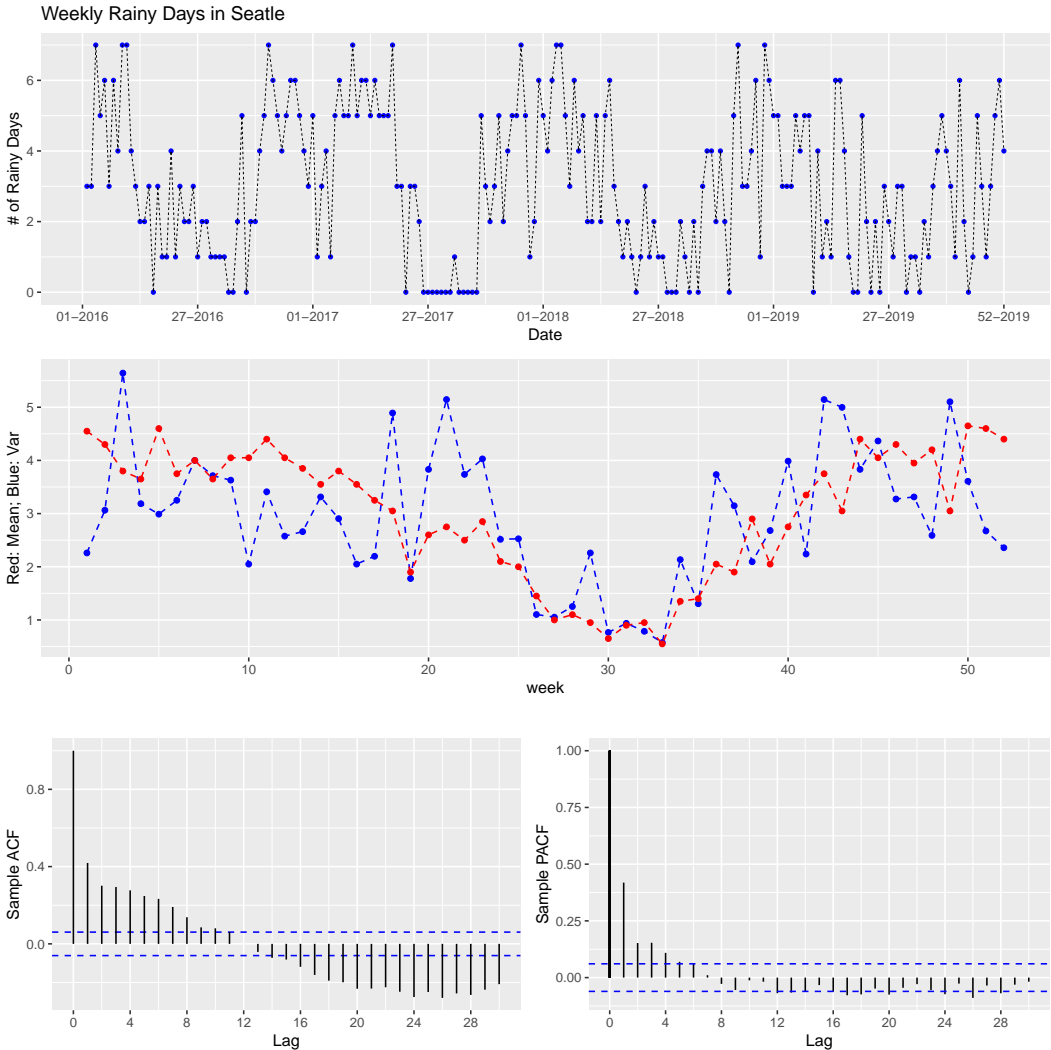


FIGURE 5 Top: The Seattle weekly rainy day counts from 2016-2019 only; Middle: Weekly sample means and variance for the rainy day counts from 2000-2019; Bottom left and bottom right: Sample ACF and PACF of all observations.

This section applies our techniques to a series of weekly rainy day counts in the Seattle, Washington area recorded from 01-Jan-2000 to 31-Dec-2019. The data were collected at the Seattle Tacoma airport weather station and are available at <http://www.ncdc.noaa.gov>. Here, any day receiving a non-zero amount of precipitation is counted as a rainy day. As such, $X_t \in \{0, 1, 2, 3, 4, 5, 6, 7\}$ for each t . For convenience, we only analyze the first 364 days in a year, inducing a period of $T = 52$ in the series. Any inaccuracies incurred by neglecting these days is minimal. Figure 3

summarizes our data. The top plot graphs the weekly rainy day counts from the last four years of the series only (for visual clarity), from the first week in 2016 to the 52nd week in 2019. One sees a clear seasonal cycle with summer weeks experiencing significantly less rain than winter weeks. The middle plot in the figure displays the sample mean and variance of the weekly counts over the entire 20 year data period, aggregated by week of year. For example, the mean and variance for the 1st week in January are the sample means and variance (denominator of 19) over all 20 1st weeks occurring from 2000 to 2019. The sample mean and variance have roughly sinusoidal structures and are minimal during the summer months. The bottom plots in the figure show sample autocorrelations (ACF) and partial autocorrelations (PACF) of the series. The pattern in the ACF is indicative of a periodic mean in the series that has not been removed.

Several marginal distributions for this series merit exploration. The binomial distribution with seven trials is a classic structure for such data. However, this distribution is underdispersed (variance is smaller than the mean), which does not jibe with the data patterns seen in the middle plot of Figure 5. Another distribution considered is the TSMC distribution of the last section. This distribution can be overdispersed, and as we will subsequently see, fits our series quite well. A final marginal distribution considered is the generalized Poisson marginal truncated to the support set $\{0, 1, 2, 3, 4, 5, 6, 7\}$. For clarity, the generalized Poisson marginal we use has distribution

$$\begin{aligned}\mathbb{P}(Y = k) &= \frac{e^{-(\lambda+\eta k)} \lambda(\lambda + \eta k)^{k-1}}{k!}, \quad k = 0, 1, \dots; \\ \mathbb{E}(Y) &= \mu = \frac{\lambda}{1-\eta}; \\ \text{Var}(Y) &= \sigma^2 = \frac{\lambda}{(1-\eta)^3}\end{aligned}$$

for a count variable Y , with $\lambda > 0$ and $\eta \in [0, 1)$. When $\eta = 0$, Y is $\text{Poisson}(\lambda)$ and is equi-dispersed. First order Fourier cosine constraints are placed on the mean and variance pair $(\mu(\nu), \sigma^2(\nu))$ and then mapped back to parameter pair $(\lambda(\nu), \alpha(\nu))$.

For structures of $\{Z_t\}$, we consider PAR(1), AR(1), and SAR(1) models (see Section 2). The PAR(1) structure uses the first order Fourier cosine consolidation in (29) for $\{Z_t\}$. The AR(1) $\{Z_t\}$ is simply a standard AR(1) series with a unit variance. The SAR(1) form for $\{Z_t\}$ is the two parameter model in Example 2.2. For parameters in the marginal distributions, the success probabilities are

$$\rho(\nu) = a_1 + a_2 \cos\left(\frac{2\pi(a_3 - \nu)}{T}\right)$$

in the binomial fits;

$$\alpha(\nu) = a_1 + a_2 \cos\left(\frac{2\pi(a_3 - \nu)}{T}\right), \quad \beta(\nu) = b_1 + b_2 \cos\left(\frac{2\pi(b_3 - \nu)}{T}\right),$$

for the TSMC fits, and

$$\begin{aligned}\mu(\nu) &= a_1 + a_2 \cos\left(\frac{2\pi(a_3 - \nu)}{T}\right), & \sigma^2(\nu) &= b_1 + b_2 \cos\left(\frac{2\pi(b_3 - \nu)}{T}\right), \\ \lambda(\nu) &= 1 - \sqrt{\frac{\mu(\nu)}{\sigma^2(\nu)}}, & \alpha(\nu) &= \mu(\nu) \sqrt{\frac{\mu(\nu)}{\sigma^2(\nu)}}\end{aligned}$$

in the truncated generalized Poisson fit.

Table 5 displays BIC and AIC scores for various fitted $\{Z_t\}$ structures and marginal distributions. The best marginal distribution is the TSMC; the truncated generalized Poisson marginal distribution is a close second. The generalized Poisson marginal distribution is known to be a very flexible count time series model (Ver Hoef and Boveng, 2007) that fits many observed series well. Of note is that an AR(1) latent $\{Z_t\}$ is preferred to either a PAR(1) or SAR(1) structure. This does not mean that the end fitted model is non-periodic; indeed, the parameters in the marginal distribution F_ν depend highly on the week of year ν . However, the seasonality in the PAR(1) and SAR(1) $\{Z_t\}$ do not make an appreciable difference – a stationary AR(1) $\{Z_t\}$ is sufficient.

Marginal Distribution	Model	WN	AR(1)	PAR(1)	SAR(1)
Binomial	AIC	4278.628	4227.775	4229.708	4229.458
	BIC	4293.469	4247.563	4259.39	4254.193
Two State Markov Chain (TSMC)	AIC	3888.114	3853.589	3856.244	3855.624
	BIC	3917.796	3888.218	3900.766	3895.200
Truncated Overdispersed Poisson	AIC	3885.032	3853.840	3856.995	3855.672
	BIC	3914.714	3888.469	3901.518	3895.248

TABLE 5 AIC and BIC statistics for models with binomial, TSMC, and truncated Poisson marginal distributions. The lowest AIC/BIC for each marginal distribution are bolded. The TSMC marginal distribution with an AR(1) $\{Z_t\}$ is judged optimal.

Table 6 shows the estimated parameters in the fitted model. Based on asymptotic normality, which is expected but has not been proven, all parameters except b_3 appear to be significantly non-zero. A zero b_3 is plausible: $b_3 = 0$ implies that the maximal variability of the weekly rainy day counts start at the beginning of the calendar year, which roughly corresponds to the meteorological height of winter. Standard errors were estimated by inverting the Fisher information matrix at the likelihood estimates. For completeness, Table 7 shows parameter estimates and standard errors for the truncated generalized Poisson fit. The interpretation of these results are similar to those above.

TABLE 6 Estimates and standard errors of the TSMC AR(1) model. The L-BFGS-B algorithm was used to optimize particle filtering likelihoods.

Parameters	a_1	a_2	a_3	b_1	b_2	b_3	ϕ
Point Estimates	0.737	-0.163	4.687	0.648	0.132	1.660	0.198
Standard Error	0.011	0.014	0.674	0.013	0.018	1.039	0.032

TABLE 7 Estimates and standard errors of the generalized Poisson-AR(1) fit. The L-BFGS-B algorithm is used to optimize particle filtering likelihoods.

Parameters	a_1	a_2	a_3	b_1	b_2	b_3	ϕ
Point Estimates	3.999	2.975	3.977	8.155	6.926	3.955	0.195
Standard Error	0.263	0.298	0.448	1.586	1.685	0.926	0.033

Moving to a residual analysis, Figure 6 shows diagnostics for the TSMC marginal with an AR(1) $\{Z_t\}$. The top

left plot shows the raw residuals and the bottom left and right plots show sample ACFs and PACFs of these residuals. No major issues are seen. The top right graph shows a QQ plot of these residuals for a standard normal distribution. Some departure from normality is noted in the two tails of the plot.

Finally, Figure 7 shows PIT histograms of the residuals for the binomial and TSMC fits with AR(1) $\{Z_t\}$. There are obvious departures from uniformity for the binomial marginal – this marginal distribution does not seem to describe the data well. The histogram for the two-state Markov chain marginal is roughly uniform; hence, we have a good fitting model and the slight lack of normality in $\{Z_t\}$ in Figure 6 does not appear overly problematic.

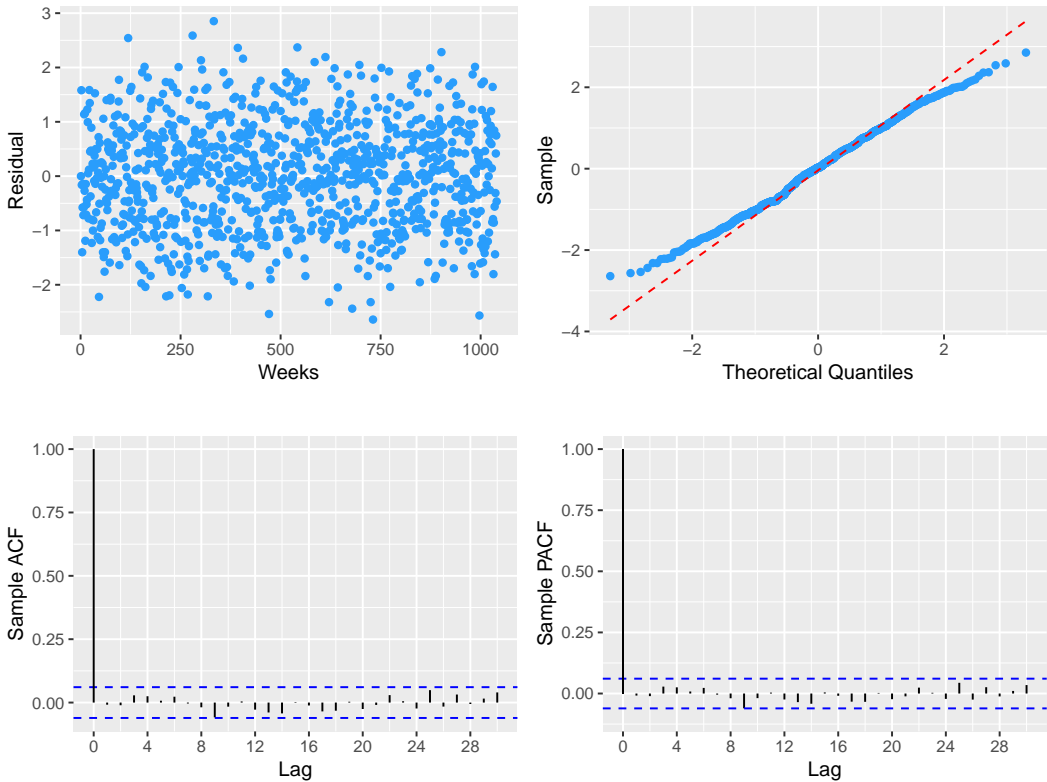


FIGURE 6 Top left: TSMC + AR(1) residuals. Top right: A QQ plot of these residuals. Bottom left: The sample ACF of these residuals. Bottom right: The sample PACF of these residuals.

7 | CONCLUDING COMMENTS

The above paper constructs a very general model for seasonal count time series through a latent Gaussian process transformation. Any marginal distribution can be achieved and the correlations are as flexible as possible and can be negative. Estimation of the model parameters through likelihood techniques can be conducted by particle filtering techniques. The methods were shown to work well on simulated data and capably handled a periodic count sequence supported on $\{0, 1, 2, 3, 4, 5, 6, 7\}$. There, we found that the latent Gaussian process did not need to be periodic,

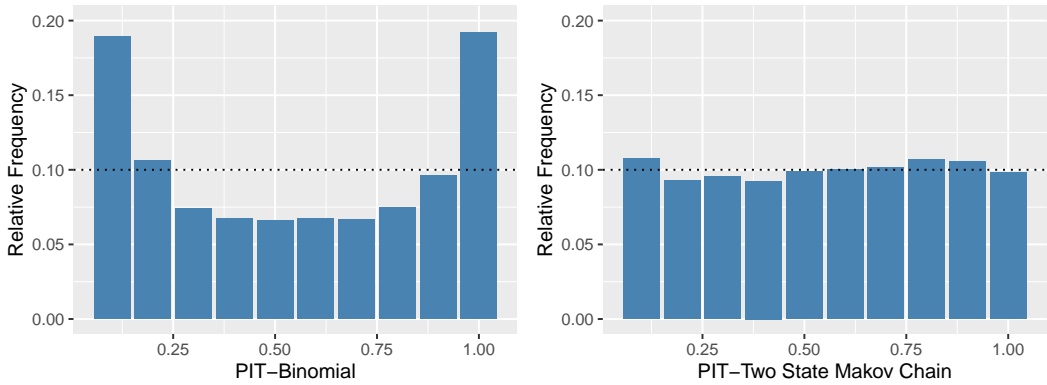


FIGURE 7 Left: a binomial marginal PIT histogram. Right: a TSMC marginal PIT histogram. The binomial marginal does not fit as well as the TSMC marginal.

but the marginal distribution of the data contained periodicities. The fitted model was very parsimonious, containing only seven parameters.

Extensions of the above techniques to handle covariates merit exploration. For this, we suggest allowing θ to depend on the covariates as in Jia et al. (2021). Trying to modify the latent Gaussian process to handle covariates generally causes trouble. Multivariate versions of the methods are also worth studying.

8 | APPENDIX

Proof of Proposition 3.1: We follow similar reasoning to Pipiras and Taqqu (2017) and Jia et al. (2021). We begin with a generalization of the Price Theorem (Theorem 5.8.5 in Pipiras and Taqqu (2017)), stated as follows and easily proven. Let G_{v_1} and G_{v_2} be two continuous differentiable functions. Then their link function has a derivative with form

$$L'(u) = \frac{1}{\sqrt{\text{Var}(X_1)\text{Var}(X_2)}} E[G'_{v_1}(Z_1)G'_{v_2}(Z_2)] \Big|_{\text{Corr}(Z_1, Z_2)=u}. \quad (32)$$

Here, Z_1 and Z_2 are a correlated Gaussian pair, each component standardized, and with $\text{Corr}(Z_1, Z_2) = u$.

In our application, G_{v_1} and G_{v_2} are non-negative and non-decreasing since they are cumulative distribution functions. But because our data are counts, G_{v_1} and G_{v_2} are step functions and not necessarily differentiable on the integers. To remedy this, we approximate G_{v_1} and G_{v_2} by differentiable functions and take limits in the approximation.

To do this, let $U \stackrel{D}{=} N(0, 1)$. For any $\epsilon > 0$ and $\ell \in \{1, 2\}$,

$$\begin{aligned}
 G_{\epsilon, \nu_\ell}(x) &:= E[G_{\nu_\ell}(x + \epsilon U)] = \int_{-\infty}^{\infty} G_{\nu_\ell}(z) \frac{e^{-\frac{(x-z)^2}{2\epsilon^2}}}{\sqrt{2\pi\epsilon}} dz \\
 &= \sum_{j=0}^{\infty} j \int_{\Phi^{-1}(C_{j-1}(\nu_\ell))}^{\Phi^{-1}(C_j(\nu_\ell))} \frac{e^{-\frac{(x-z)^2}{2\epsilon^2}}}{\sqrt{2\pi\epsilon}} dz \\
 &= \sum_{j=0}^{\infty} j \int_{\Phi^{-1}(C_{j-1}(\nu_\ell)) - x}^{\Phi^{-1}(C_j(\nu_\ell)) - x} \frac{e^{-\frac{w^2}{2\epsilon^2}}}{\sqrt{2\pi\epsilon}} dw. \tag{33}
 \end{aligned}$$

The “kernel”

$$\frac{e^{-\frac{(x-z)^2}{2\epsilon^2}}}{\sqrt{2\pi\epsilon}} \tag{34}$$

acts like Dirac's delta function $\delta_{\{x\}}(z)$ at $z = x$ as $\epsilon \downarrow 0$. Note that $G_{\epsilon, \nu_\ell}(x)$ is non-decreasing and differentiable with first derivative

$$G'_{\epsilon, \nu_\ell}(x) = \frac{1}{\sqrt{2\pi\epsilon}} \sum_{j=0}^{\infty} j \left[e^{-\frac{(\Phi^{-1}(C_{j-1}(\nu_\ell)) - x)^2}{2\epsilon^2}} - e^{-\frac{(\Phi^{-1}(C_j(\nu_\ell)) - x)^2}{2\epsilon^2}} \right] = \frac{1}{\sqrt{2\pi\epsilon}} \sum_{j=0}^{\infty} e^{-\frac{(\Phi^{-1}(C_j(\nu_\ell)) - x)^2}{2\epsilon^2}}, \tag{35}$$

and define $X_\ell^{(\epsilon)} = G_{\epsilon, \nu_\ell}(Z_\ell)$ for $\ell \in \{1, 2\}$. Equation (15) gives

$$\begin{aligned}
 L'_\epsilon(u) &= \frac{1}{\sqrt{\text{Var}(X_1^{(\epsilon)})\text{Var}(X_2^{(\epsilon)})}} E[G'_{\epsilon, \nu_1}(Z_1)G'_{\epsilon, \nu_2}(Z_2)] \Big|_{\text{Corr}(Z_1, Z_2)=u} \\
 &= \frac{1}{\sqrt{\text{Var}(X_1^{(\epsilon)})\text{Var}(X_2^{(\epsilon)})}} \int_{-\infty}^{\infty} \int_{-\infty}^{\infty} G'_{\epsilon, \nu_1}(Z_1)G'_{\epsilon, \nu_2}(Z_2) \frac{1}{2\pi\sqrt{1-u^2}} e^{-\frac{1}{2(1-u^2)}(z_1^2+z_2^2-2uz_1z_2)} dz_1 dz_2 \\
 &= \frac{1}{\sqrt{\text{Var}(X_1^{(\epsilon)})\text{Var}(X_2^{(\epsilon)})}} \sum_{j_1=0}^{\infty} \sum_{j_2=0}^{\infty} \int_{-\infty}^{\infty} \int_{-\infty}^{\infty} \frac{1}{\sqrt{2\pi\epsilon}} e^{-\frac{(\Phi^{-1}(C_{j_1}(\nu_1)) - z_1)^2}{2\epsilon^2}} \frac{1}{\sqrt{2\pi\epsilon}} e^{-\frac{(\Phi^{-1}(C_{j_2}(\nu_2)) - z_2)^2}{2\epsilon^2}} \times \\
 &\quad \frac{1}{2\pi\sqrt{1-u^2}} e^{-\frac{1}{2(1-u^2)}(z_1^2+z_2^2-2uz_1z_2)} dz_1 dz_2. \tag{36}
 \end{aligned}$$

Noting again that the quantity in (34) acts like a Dirac's delta function $\delta_{\{x\}}(z)$, the limit as $\epsilon \downarrow 0$ should be

$$L'(u) = \frac{1}{\sqrt{\text{Var}(X_1)\text{Var}(X_2)}} \sum_{j_1=0}^{\infty} \sum_{j_2=0}^{\infty} \frac{1}{2\pi\sqrt{1-u^2}} e^{-\frac{1}{2(1-u^2)}(\Phi^{-1}(C_{j_1}(\nu_1))^2 + \Phi^{-1}(C_{j_2}(\nu_2))^2 - 2u\Phi^{-1}(C_{j_1}(\nu_1))\Phi^{-1}(C_{j_2}(\nu_2))}), \tag{37}$$

which is always non-negative. The existence and form of $L'(u)$ stems from the fact that we are differentiating a power series with absolutely convergent coefficients inside its radius of convergence. That $\sum_{k=0}^{\infty} |\ell_k| < \infty$ follows from (14), the Cauchy-Schwarz inequality, and the finiteness of $\sum_{k=0}^{\infty} k!g_k(\nu_1)^2$ and $\sum_{k=0}^{\infty} k!g_k(\nu_2)^2$.

We now show that $L'_\epsilon(u)$ converges to $L'(u)$. For this, we first need an expression for the Hermite coefficients of $G_{\epsilon, \nu_\ell}(\cdot)$, denoted by $g_{\epsilon, k}(\nu_\ell)$ for $\ell \in \{1, 2\}$. These will be compared to the Hermite coefficients $g_k(\nu_\ell)$ of G_{ν_ℓ} .

Taylor expanding the Hermite polynomial $H_k(x+y) = \sum_{d=0}^k \binom{k}{d} y^{k-d} H_d(x)$ implies

$$\begin{aligned} G_{\epsilon, v_\ell}(x) &= E[G_{v_\ell}(x + \epsilon U)] = E\left[\sum_{k=0}^{\infty} g_k(v_\ell) H_k(x + \epsilon U)\right] \\ &= E\left[\sum_{k=0}^{\infty} g_k(v_\ell) \sum_{d=0}^k \binom{k}{d} (\epsilon U)^{k-d} H_d(x)\right] \\ &= \sum_{d=0}^{\infty} H_d(x) \sum_{k=d}^{\infty} g_k(v_\ell) \epsilon^{k-d} \binom{k}{d} E[U^{k-d}]. \end{aligned}$$

After changing summation indices and using that $E[U^p] = 0$ if p is odd, and equal to $(p-1)!!$ if p is even, where $k!! = 1 \times 3 \times \dots \times k$ when k is odd, we get

$$g_{\epsilon, k}(v_\ell) = g_k(v_\ell) + \sum_{q=1}^{\infty} g_{k+2q}(v_\ell) \epsilon^{2q} \binom{k+2q}{k} (2q-1)!! = g_k(v_\ell) + \sum_{q=1}^{\infty} g_{k+2q}(v_\ell) \epsilon^{2q} \frac{(k+2q)!}{k! 2^q q!}. \quad (38)$$

Then

$$\begin{aligned} |g_k(v_1)g_k(v_2) - g_{\epsilon, k}(v_1)g_{\epsilon, k}(v_2)| &\leq |g_k(v_1)| \sum_{q=1}^{\infty} |g_{k+2q}(v_1)| \epsilon^{2q} \frac{(k+2q)!}{k! 2^q q!} + |g_k(v_2)| \sum_{q=1}^{\infty} |g_{k+2q}(v_2)| \epsilon^{2q} \frac{(k+2q)!}{k! 2^q q!} \\ &\quad + \left(\sum_{q=1}^{\infty} |g_{k+2q}(v_1)| \epsilon^{2q} \frac{(k+2q)!}{k! 2^q q!}\right) \left(\sum_{q=1}^{\infty} |g_{k+2q}(v_2)| \epsilon^{2q} \frac{(k+2q)!}{k! 2^q q!}\right). \end{aligned} \quad (39)$$

Use the Cauchy-Schwarz inequality to obtain the bounds

$$\begin{aligned} \sum_{q=1}^{\infty} |g_{k+2q}(v_\ell)| \epsilon^{2q} \frac{(k+2q)!}{k! 2^q q!} &\leq \left(\sum_{q=1}^{\infty} g_{k+2q}^2(v_\ell) (k+2q)!\right)^{1/2} \left(\sum_{q=1}^{\infty} \epsilon^{4q} \frac{(k+2q)!}{(k!)^2 (2^q q!)^2}\right)^{1/2} \\ &\leq \frac{M_{k, \ell}}{(k!)^{1/2}} \left(\sum_{q=1}^{\infty} \epsilon^{4q} \frac{(k+2q)!}{k! (2^q q!)^2}\right)^{1/2} \quad \forall \ell \in \{1, 2\}, \end{aligned}$$

where $M_{k, \ell}$ is some finite constant that converges to zero as $k \rightarrow \infty$. Since $\text{Var}(X_\ell) = \sum_{k=1}^{\infty} k! g_k^2(v_\ell)$ is finite and $(2^q q!)^2$ is of the same order as $(2q)!$, $\sum_{q=1}^{\infty} g_{k+2q}^2(v_\ell) (k+2q)! \rightarrow 0$ as $k \rightarrow \infty$. We use the fact that $\sum_{p=0}^{\infty} x^p \binom{k+p}{p} = (1-x)^{-k-1}$ for $|x| < 1$ to obtain a bound for $\sum_{p=1}^{\infty} \epsilon^{2p} \binom{k+p}{p}$. Then (39) gives

$$|g_k(v_1)g_k(v_1) - g_{\epsilon, k}(v_1)g_{\epsilon, k}(v_2)| \leq \sum_{\ell=1}^2 \frac{M_{k, \ell} |g_k(v_\ell)|}{(k!)^{1/2}} \left[(1 - \epsilon^2)^{-k-1} - 1\right]^{1/2} + \frac{M_{k, 1} M_{k, 2}}{k!} \left[(1 - \epsilon^2)^{-k-1} - 1\right]. \quad (40)$$

Now take the first derivative of the link function in (13) to obtain

$$L'(u) = \frac{1}{\sqrt{\text{Var}(X_1)\text{Var}(X_2)}} \sum_{k=1}^{\infty} g_k(v_1)g_k(v_2) k! k u^{k-1},$$

where the series converges absolutely for $u \in (-1, 1)$ since the “extra” k gets dominated by u^{k-1} . Similarly,

$$L'_\epsilon(u) = \frac{1}{\sqrt{\text{Var}(X_1)\text{Var}(X_2)}} \sum_{k=1}^{\infty} g_{\epsilon,k}(v_1)g_{\epsilon,k}(v_2)k!k|u|^{k-1}.$$

The above expression agrees with Theorem 5.1.10 in Pipiras and Taqqu (2017). To show that the difference between $L'_\epsilon(u)$ and $L'(u)$ converges to zero as $\epsilon \downarrow 0$, use

$$\begin{aligned} |L'(u) - L'_\epsilon(u)| &\leq \left| \frac{1}{\sqrt{\text{Var}(X_1)\text{Var}(X_2)}} - \frac{1}{\sqrt{\text{Var}(X_1^{(\epsilon)})\text{Var}(X_2^{(\epsilon)})}} \right| \sum_{k=1}^{\infty} g_k(v_1)g_k(v_2)k!k|u|^{k-1} \\ &+ \frac{1}{\sqrt{\text{Var}(X_1^{(\epsilon)})\text{Var}(X_2^{(\epsilon)})}} \sum_{k=1}^{\infty} |g_k(v_1)g_k(v_2) - g_{\epsilon,k}(v_1)g_{\epsilon,k}(v_2)|k!k|u|^{k-1}. \end{aligned} \quad (41)$$

From (40), we see that $|g_k(v_1)g_k(v_2) - g_{\epsilon,k}(v_1)g_{\epsilon,k}(v_2)| \rightarrow 0$ as $\epsilon \downarrow 0$. Hence, $\sum_{k=1}^{\infty} |g_k(v_1)g_k(v_2) - g_{\epsilon,k}(v_1)g_{\epsilon,k}(v_2)|k!k|u|^{k-1}$ converges to zero by the dominated convergence theorem as $\epsilon \downarrow 0$. Using (12), we concluded that $\text{Var}(X_1^{(\epsilon)}) \rightarrow \text{Var}(X_1)$ and $\text{Var}(X_2^{(\epsilon)}) \rightarrow \text{Var}(X_2)$ as $\epsilon \downarrow 0$. Therefore,

$$\left| \frac{1}{\sqrt{\text{Var}(X_1)\text{Var}(X_2)}} - \frac{1}{\sqrt{\text{Var}(X_1^{(\epsilon)})\text{Var}(X_2^{(\epsilon)})}} \right| \rightarrow 0 \quad \text{as } \epsilon \downarrow 0$$

follows by continuity of the function $x^{-1/2}$ away from $x = 0$ (the limiting variances are tacitly assumed positive to avoid degeneracy).

references

- Aknouche, A., W. Bentarzi, and N. Demouche, 2018: On periodic ergodicity of a general periodic mixed Poisson autoregression. *Statistics & Probability Letters*, **134**, 15–21.
- Anderson, P. L., Y. G. Tesfaye, and M. M. Meerschaert, 2007: Fourier-PARMA models and their application to river flows. *Journal of Hydrologic Engineering*, **12**, no. 5, 462–472.
- Asmussen, S. and S. Foss, 2014: On exceedance times for some processes with dependent increments. *Journal of Applied Probability*, **51**, no. 1, 136–151.
- Bai, Y., J. Kang, and P. X.-K. Song, 2014: Efficient pairwise composite likelihood estimation for spatial-clustered data. *Biometrics*, **70**, no. 3, 661–670.
- Basawa, I. and R. Lund, 2001: Large sample properties of parameter estimates for periodic ARMA models. *Journal of Time Series Analysis*, **22**, no. 6, 651–663.
- Basawa, I., R. Lund, and Q. Shao, 2004: First-order seasonal autoregressive processes with periodically varying parameters. *Statistics & Probability Letters*, **67**, no. 4, 299–306.
- Bentarzi, M. and N. Aries, 2020: On some periodic INARMA (p, q) models. *Communications in Statistics-Simulation and Computation*, 1–21.
- Bentarzi, M. and W. Bentarzi, 2017: Periodic integer-valued bilinear time series model. *Communications in Statistics-Theory and Methods*, **46**, no. 3, 1184–1201.

- Bloomfield, P., H. L. Hurd, and R. B. Lund, 1994: Periodic correlation in stratospheric ozone data. *Journal of Time Series Analysis*, **15**, no. 2, 127–150.
- Brockwell, P. J. and R. A. Davis, 1991: *Time Series: Theory and Methods*. 2nd ed., Springer.
- Chatfield, C. and D. Prothero, 1973: Box-Jenkins seasonal forecasting: problems in a case-study. *Journal of the Royal Statistical Society: Series A*, **136**, no. 3, 295–315.
- Czado, C., T. Gneiting, and L. Held, 2009: Predictive model assessment for count data. *Biometrics*, **65**, no. 4, 1254–1261.
- Davis, R. A., K. Fokianos, S. H. Holan, H. Joe, J. Livsey, R. Lund, V. Pipiras, and N. Ravishanker, 2021: Count time series: A methodological review. *Journal of the American Statistical Association*, **116**, 1533–1547.
- Davis, R. A., S. H. Holan, R. Lund, and N. Ravishanker, 2016: *Handbook of Discrete-Valued Time Series*. CRC Press, New York City, NY.
- Dawid, A. P., 1984: Present position and potential developments: Some personal views statistical theory the prequential approach. *Journal of the Royal Statistical Society: Series A*, **147**, no. 2, 278–290.
- Fokianos, K., 2012: Count time series models. *Handbook of Statistics*, C. R. Rao, C. Rao, and V. Govindaraju, Eds., Elsevier, volume 30, 315–347.
- Fralix, B., J. Livsey, and R. Lund, 2012: Renewal sequences with periodic dynamics. *Probability in the Engineering and Informational Sciences*, **26**, no. 1, 1–15.
- Franses, P. H., 1994: A multivariate approach to modeling univariate seasonal time series. *Journal of Econometrics*, **63**, no. 1, 133–151.
- Franses, P. H. and R. Paap, 2004: *Periodic Time Series Models*. Oxford University Press.
- Gardner, W. and L. Franks, 1975: Characterization of cyclostationary random signal processes. *IEEE Transactions on Information Theory*, **21**, no. 1, 4–14.
- Gardner, W. A., A. Napolitano, and L. Paura, 2006: Cyclostationarity: Half a century of research. *Signal Processing*, **86**, no. 4, 639–697.
- Genz, A. and F. Bretz, 2002: Comparison of methods for the computation of multivariate t probabilities. *Journal of Computational and Graphical Statistics*, **11**, no. 4, 950–971.
- Geweke, J., 1991: Efficient simulation from the multivariate normal and student- t distributions subject to linear constraints and the evaluation of constraint probabilities. *Computing Science and Statistics: Proceedings of the 23rd Symposium on the Interface*, Citeseer, volume 571, 578.
- Glasserman, P. and D. D. Yao, 1992: Some guidelines and guarantees for common random numbers. *Management Science*, **38**, no. 6, 884–908.
- Hajivassiliou, V., D. McFadden, and P. Ruud, 1996: Simulation of multivariate normal rectangle probabilities and their derivatives theoretical and computational results. *Journal of Econometrics*, **72**, no. 1-2, 85–134.
- Han, Z. and V. De Oliveira, 2016: On the correlation structure of Gaussian copula models for geostatistical count data. *Australian & New Zealand Journal of Statistics*, **58**, no. 1, 47–69.
- 2018: gcKrig: An R package for the analysis of geostatistical count data using Gaussian copulas. *Journal of Statistical Software*, **87**, no. 1, 1–32.
- 2020: Maximum likelihood estimation of Gaussian copula models for geostatistical count data. *Communications in Statistics-Simulation and Computation*, **49**, no. 8, 1957–1981.

- Hurd, H. L. and A. Miamee, 2007: *Periodically Correlated Random Sequences: Spectral Theory and Practice*, volume 355. John Wiley & Sons.
- Jia, Y., S. Kechagias, J. Livsey, R. Lund, and V. Pipiras, 2021: Latent Gaussian count time series. *Journal of the American Statistical Association*, **To appear**.
- Joe, H., 2016: Markov models for count time series. *Handbook of Discrete-Valued Time Series*, R. A. Davis, S. H. Holan, R. Lund, and N. Ravishanker, Eds., CRC Press, New York City, NY, 49–70.
- 2019: Likelihood inference for generalized integer autoregressive time series models. *Econometrics*, **7**, no. 4.
- Kachour, M. and J.-F. Yao, 2009: First-order rounded integer-valued autoregressive (RINAR (1)) process. *Journal of Time Series Analysis*, **30**, no. 4, 417–448.
- Kazianka, H., 2013: Approximate copula-based estimation and prediction of discrete spatial data. *Stochastic Environmental Research and Risk Assessment*, **27**, no. 8, 2015–2026.
- Kazianka, H. and J. Pilz, 2010: Copula-based geostatistical modeling of continuous and discrete data including covariates. *Stochastic Environmental Research and Risk Assessment*, **24**, no. 5, 661–673.
- Kleinman, N. L., J. C. Spall, and D. Q. Naiman, 1999: Simulation-based optimization with stochastic approximation using common random numbers. *Management Science*, **45**, no. 11, 1570–1578.
- Livsey, J., R. Lund, S. Kechagias, V. Pipiras, et al., 2018: Multivariate integer-valued time series with flexible autocovariances and their application to major hurricane counts. *The Annals of Applied Statistics*, **12**, no. 1, 408–431.
- Lund, R., 2011: Choosing seasonal autocovariance structures: PARMA or SARMA. *Economic Time Series: Modelling and Seasonality*, W. R. Bell, S. H. Holan, and T. S. McElroy, Eds., Chapman and Hall/CRC, 63–80.
- Lund, R. and I. Basawa, 1999: Modeling and inference for periodically correlated time series. *Asymptotics, Nonparametrics, and Time Series*, S. Ghosh, ed., CRC Press, 37–52.
- 2000: Recursive prediction and likelihood evaluation for periodic ARMA models. *Journal of Time Series Analysis*, **21**, no. 1, 75–93.
- Lund, R., H. Hurd, P. Bloomfield, and R. Smith, 1995: Climatological time series with periodic correlation. *Journal of Climate*, **8**, no. 11, 2787–2809.
- Lund, R. and J. Livsey, 2016: Renewal-based count time series. *Handbook of Discrete-Valued Time Series*, R. A. Davis, S. H. Holan, R. Lund, and N. Ravishanker, Eds., CRC Press, New York City, NY.
- Lund, R., Q. Shao, and I. Basawa, 2006: Parsimonious periodic time series modeling. *Australian & New Zealand Journal of Statistics*, **48**, no. 1, 33–47.
- Masarotto, G., C. Varin, et al., 2017: Gaussian copula regression in R. *Journal of Statistical Software*, **77**, no. 8, 1–26.
- Monteiro, M., M. G. Scotto, and I. Pereira, 2010: Integer-valued autoregressive processes with periodic structure. *Journal of Statistical Planning and Inference*, **140**, no. 6, 1529–1541.
- 2015: A periodic bivariate integer-valued autoregressive model. *Dynamics, Games and Science: International Conference and Advanced School Planet Earth, DGS II, Portugal, August 28–September 6, 2013*, J.-P. Bourguignon, R. Jeltsch, A. A. Pinto, and M. Viana, Eds., Springer, 455–477.
- Moriña, D., P. Puig, J. Ríos, A. Vilella, and A. Trilla, 2011: A statistical model for hospital admissions caused by seasonal diseases. *Statistics in Medicine*, **30**, no. 26, 3125–3136.

- Ouzzani, F. and M. Bentarzi, 2019: On mixture periodic integer-valued ARCH models. *Communications in Statistics-Simulation and Computation*, 1–27.
- Pipiras, V. and M. S. Taqqu, 2017: *Long-range Dependence and Self-similarity*, volume 45. Cambridge University Press.
- Reinsel, G. C., 2003: *Elements of Multivariate Time Series Analysis*. Springer Science & Business Media.
- Santos, C., I. Pereira, and M. Scotto, 2019: Periodic INAR(1) models with Skellam-distributed innovations. *International Conference on Computational Science and Its Applications*, Springer, 64–78.
- Santos, C., I. Pereira, and M. G. Scotto, 2021: On the theory of periodic multivariate INAR processes. *Statistical Papers*, **62**, 1291–1348.
- Shao, Q., 2006: Mixture periodic autoregressive time series models. *Statistics & Probability Letters*, **76**, no. 6, 609–618.
- Shao, Q. and R. B. Lund, 2004: Computation and characterization of autocorrelations and partial autocorrelations in periodic ARMA models. *Journal of Time Series Analysis*, **25**, 359–372.
- Shao, Q. and P. Ni, 2004: Least-squares estimation and ANOVA for periodic autoregressive time series. *Statistics & Probability Letters*, **69**, no. 3, 287–297.
- Steenbergen, M. R., 2006: Maximum likelihood programming in R. University of North Carolina, Chapel Hill. Department of Political Science.
- Tesfaye, Y. G., M. M. Meerschaert, and P. L. Anderson, 2004: Identification of PARMA models and their application to the modeling of river flows. *AGU Spring Meeting Abstracts*, volume 2004, H33A–10.
- Vecchia, A., 1985: Periodic autoregressive-moving average (PARMA) modeling with applications to water resources. *Journal of the American Water Resources Association*, **21**, no. 5, 721–730.
- Ver Hoef, J. M. and P. L. Boveng, 2007: Quasi-Poisson vs. negative binomial regression: how should we model overdispersed count data? *Ecology*, **88**, no. 11, 2766–2772.
- Wei, C. H., 2018: *An Introduction to Discrete-Valued Time Series*. John Wiley & Sons.
- Whitt, W., 1976: Bivariate distributions with given marginals. *The Annals of Statistics*, **4**, no. 6, 1280–1289.